The behaviour of highly siderophile elements in oceanic crust during subduction: whole-rock and mineral-scale insights from a high-pressure terrain

C.W. Dale[a,b*], K.W. Burton[b∞], D.G. Pearson[a], A. Gannoun[b∞], O. Alard[b#], T.W. Argles[b], I.J. Parkinson[b]

[a]*Department of Earth Sciences, Durham University, Science Laboratories, Durham, DH1 3LE, UK*

[b]*Department of Earth Sciences, CEPSAR, The Open University, Walton Hall, Milton Keynes, MK7 6AA, UK*

[∞] *current address: Dept of Earth Sciences, Oxford University, Oxford, OX1 3PR, UK*

 # current address: Univ Montpellier 2, CNRS, UMR 5243, CC 60, F-34095 Montpellier, France

[*]corresponding author. email: christopher.dale@durham.ac.uk. Tel: +44 0191 3342338, Fax: +44 0191 3342301

ABSTRACT

Highly siderophile element concentrations (HSE: Re and platinum-group elements (PGE)) are presented for gabbros and gabbroic eclogites and basaltic eclogites from the high-pressure Zermatt-Saas ophiolite terrain, Switzerland. Rhenium and PGE (Os, Ir, Ru, Pt, Pd) abundances in gabbro- and eclogite-hosted sulphides, and Re-Os isotopes and elemental concentrations in silicate phases are also reported. This work, therefore, provides whole-rock and mineral-scale insights into the PGE budget of gabbroic oceanic crust and the effects of subduction metamorphism on gabbroic and basaltic crust.

Chondrite-normalised PGE patterns for the gabbros are similar to published mid-ocean ridge basalts (MORB), but show less inter-element fractionation. Mean Pt and Pd contents of 360 and 530 pg/g, respectively, are broadly comparable to MORB, but gabbros have somewhat higher abundances of Os, Ir and Ru (mean: 64, 57 and 108 pg/g). Transformation to eclogite has not significantly changed the concentrations of the PGE, except Pd which is severely depleted in gabbroic eclogites relative to gabbros (~75% loss). In contrast, basaltic eclogites display significant depletion of Pt (≥60%), Pd (>85%) and Re (50-60%) compared with published MORB, while Os, Ir and Ru abundances are broadly comparable. Thus, these data suggest that only Pt, Pd and Re, and not Os, Ir and Ru, may be significantly fluxed into the mantle wedge from mafic oceanic crust. Re-Os model ages for gabbroic and gabbroic eclogite minerals are close to age estimates for igneous crystallisation and high-pressure metamorphism, respectively, hence the HSE budgets can be related to both igneous and metamorphic behaviour. The gabbroic budget of Os, Ir, Ru and Pd (but not Pt) is dominated by sulphide, which typically hosts >90% of the Os, whereas silicates account for most of the Re (with up to 75% in plagioclase alone). Sulphides in gabbroic eclogites tend to host a smaller proportion of the total Os (10-90%) while silicates are important hosts, probably

reflecting Os inheritance from precursor phases. Garnet contains very high Re concentrations and may account for >50% of Re in some samples. The depletion of Pd in gabbroic eclogites appears linked, at least in part, to the loss of Ni-rich sulphide.

Both basaltic and gabbroic oceanic crust have elevated Pt/Os ratios, but Pt/Re ratios are not sufficiently high to generate the coupled ^{186}Os-^{187}Os enrichments observed in some mantle melts, even without Pt loss from basaltic crust. However, the apparent mobility of Pt and Re in slab fluids provides an alternative mechanism for the generation of Pt- and Re-rich mantle material, recently proposed as a potential source of ^{187}Os-^{186}Os enrichment.

Keywords: platinum-group elements (PGE), rhenium, osmium, gabbro, MORB, oceanic crust, subduction, recycling, metasomatism, element mobility, sulphide and silicate minerals.

1. INTRODUCTION

The platinum group elements (PGE: Os, Ir, Ru, Rh, Pt, and Pd) and Re are highly siderophile elements (HSE) that provide key information on the differentiation of the early Earth and the subsequent evolution of the silicate mantle. During core-mantle separation, the 'metal-loving' siderophile elements are strongly partitioned into the metallic core, leaving a highly depleted silicate mantle. However, actual mantle siderophile element abundances are much higher than might be expected for low pressure-temperature (P-T) metal-silicate equilibration (Borisov et al., 1994; Righter and Drake, 1997; Ertel et al., 1999; Holzheid et al., 2000), most likely due to high P-T silicate-metal equilibration or heterogeneous accretion (the so-called late veneer, Chou, 1978), where continued accretion of meteoritic material, after core formation, replenished the HSE.

The HSE are also chalcophile ('sulphur-loving') and hence strongly partitioned into sulphide minerals in the silicate mantle itself. Sulphide is generally thought to be a residual phase during moderate mantle melting (e.g. <20%, during the generation of Mid-Ocean Ridge Basalts (MORB)), and those melts are also commonly sulphur saturated prior to or during eruption, resulting in sulphide crystallisation during magmatic differentiation (e.g. Lorand et al., 1999; Luguet et al., 2003; Bezos et al., 2005). Thus, the HSE are preferentially retained in residual sulphide in the mantle during melting, and further removed from such melts during the crystallisation and segregation of magmatic sulphide. Available data indicate that during magmatic crystallisation sulphide/melt partition coefficients are of a similar order of magnitude for all of the PGE (e.g. Peach et al., 1990; Fleet et al., 1996). In contrast, experimental and natural observations of mantle sulphides suggests that they melt incongruently releasing a Cu-Ni rich sulphide melt, and leaving a refractory Fe-Ni monosulphide solid solution that concentrates Os, Ir and Ru, relative to Pt, Pd and Re (e.g.

Alard et al., 2000; Bockrath et al., 2004; Peregoedova et al., 2004). Thus, the HSE variations in MORB are consistent with the widely accepted order of decreasing compatibility, from highly compatible for Os and Ir, through Ru, Pt, and Pd, to moderately incompatible for Re (e.g. Barnes et al., 1985).

Amongst the HSE, Re and Os are linked through β-decay of ^{187}Re to ^{187}Os. Due to the marked difference in compatibility during mantle melting, both oceanic and continental crust possess very high Re/Os ratios relative to the silicate mantle, and over time evolve to radiogenic Os isotope compositions. Consequently, the Re-Os isotope system potentially serves as an exceptional tracer of recycled crustal material in the convective mantle. However, recent studies have shown that during high-pressure (eclogite-facies) metamorphism accompanying subduction, Re and Os exhibit differential mobility between different rock types in the oceanic crust. Basalts show evidence for significant Re mobility and loss (50-60%, Becker, 2000; Dale et al., 2007) whereas gabbros preserve Re-Os isotope signatures consistent with little mobility of either element subsequent to igneous crystallisation (Dale et al., 2007). Such differential behaviour most likely relates to the degree of hydration of the original rock type and its deformation history, but variable behaviour of the mineral assemblage, particularly sulphides (the principal host for many HSE), may also play a role. However, the distribution and behaviour of other platinum-group elements (PGE) in the oceanic crust (both gabbro and basalt) remain poorly constrained (cf. Lorand and Juteau, 2000), as does their behaviour during high-pressure metamorphism accompanying subduction, and it is not clear to what extent HSE abundances in the silicate mantle may be affected by the recycling of oceanic crust, and in particular the extent to which Pt and Re mobility could potentially generate coupled ^{186}Os-^{187}Os enrichments observed in some mantle melts.

105 This study presents HSE abundances and Re-Os isotope data for basalts and gabbros from the
106 Zermatt-Saas ophiolite, metamorphosed to eclogite-facies conditions during the Alpine
107 orogeny. This includes whole rock and mineral data (silicate, oxide and sulphide) for
108 gabbroic eclogites and their un-metamorphosed igneous precursors, and whole rock data for
109 basaltic eclogites. As no precursor basalt has been preserved, basaltic eclogite data have been
110 compared to MORB. These results provide the first insight into the distribution of HSE in
111 gabbroic and basaltic crust (and amongst gabbroic minerals) and their behaviour during high
112 pressure metamorphism, with the potential consequences for their redistribution in the
113 subduction zone environment and recycling into the mantle.

114 ## 2. GEOLOGICAL SETTING, SAMPLE PETROGRAPHY and P-T

115 ## ESTIMATES (smaller type possible)

116 Samples were collected from the Zermatt-Saas ophiolite (ZSO), Switzerland, which originally
117 formed part of the Mesozoic Tethyan oceanic crust (~164 Ma, Rubatto et al., 1998). The ZSO
118 underwent Eocene high- to ultra-high pressure (UHP) metamorphism during south-easterly
119 directed subduction and the subsequent continental collision that formed the Alpine mountain
120 belt. Sampling of the variably metamorphosed Allalin Gabbro body and nearby metabasaltic
121 eclogite units (Täschalp-Pfulwe) was aimed at retrieving lithologies representative of the
122 mafic lower and upper oceanic crust, much of which was recrystallised under metamorphic
123 conditions comparable to those present in subduction zones. Details of sampling area and
124 localities can be found in Dale et al. (2007).

125

126 **2.1 Petrology and silicate mineralogy**

127 Samples of gabbroic origin preserve a range of *apparent* metamorphic conditions, although
128 field (and even hand-specimen) evidence indicates that all parts of the Allalin unit
129 experienced similar eclogite-facies P-T conditions. In some cases, the magmatic mineralogy
130 of the gabbros, principally forsterite-rich olivine, augite and labradoritic plagioclase
131 (compositions in Table EA-1, electronic annex), is preserved entirely. This metastable
132 preservation probably results from the local absence of fluid infiltration, anhydrous
133 mineralogy and a relatively low peak temperature (~600°C, see below). In contrast, other
134 samples from the same body have recrystallised entirely during metamorphism and comprise
135 an eclogite-facies mineralogy (including garnet, omphacite, zoisite, paragonite, talc and
136 glaucophane, Table EA-1). Although a complex spectrum exists, most gabbros and gabbroic
137 eclogites chosen for this study represent the two endmembers. However, several samples
138 from the Allalin Gabbro display a transition from gabbro to metagabbro/eclogite on the scale
139 of an individual hand specimen (referred to as transitional gabbros). These samples probably
140 experienced some fluid infiltration and recrystallisation during seafloor metamorphism (see
141 below) and further recrystallisation during HP metamorphism, but both transformations are
142 incomplete. The utility of such samples, and this gabbroic body as a whole, is the opportunity
143 to directly compare the chemistry of unmodified gabbros with genetically-related eclogite
144 equivalents, without the uncertainties that typically arise when comparing igneous materials
145 with differing sources and magmatic history.

146 Little or no greenschist-facies retrogression is evident in the gabbroic eclogites chosen.
147 Samples were not taken from the more deformed edges of the Allalin body, which display
148 greater retrogression, and consequently the sample suite may have a bias towards less
149 deformed samples which may have experienced less fluid flow during prograde

150 metamorphism. However, all eclogites experienced fluid infiltration, probably initially during
151 seafloor alteration (oxygen isotope evidence, Barnicoat and Cartwright, 1997). Basaltic
152 eclogites consist entirely of metamorphic minerals: garnet, omphacite, zoisite, glaucophane,
153 phengite +/- paragonite, and retrograde barroisitic amphibole. Some of the metabasalts
154 display variable greenschist retrogression (<20%), but it is considered unlikely that the
155 samples have been extensively chemically modified during exhumation.

156 **2.2 Sulphide and oxide mineralogy**

157 Accessory oxides and sulphides combined constitute less than 2% of each whole rock.
158 Ilmenite and Al-chromite (variable Cr number: 0.46 and 0.74 in two different samples) are
159 present in most of the gabbros studied, while both are absent from the gabbroic eclogites. An
160 Fe-rich sulphide (pyrrhotite, Po), Ni-rich sulphide (pentlandite, Pn) and Cu-rich sulphide
161 (chalcopyrite, Cp) are all present in the gabbros, with pyrrhotite constituting 60-90% of total
162 sulphide in the three samples for which PGE in sulphide have been determined (e.g. Figure 1).
163 Some (original?) pyrrhotite has been altered to troilite which, combined with Fe-rich
164 pentlandite and chalcopyrite, may suggest a degree of alteration under mildly reducing
165 conditions (Lorand, 1985). Pentlandite and chalcopyrite occur in modal proportions of ~10-
166 30% and <10%, respectively. An important distinction in sulphide mineralogy is the
167 predominance of pyrite in the gabbroic eclogites (50-100%), and its absence in the gabbros.
168 Pyrrhotite and chalcopyrite are also present in the gabbroic eclogites, but are much less
169 common (1-45% and <5%, respectively), while pentlandite is absent. Typical major element
170 compositions of the sulphide phases are given in Table 1.

171 Figure 1 here.

172 Table 1 here.

Gabbroic sulphides range in diameter from 1 to 500 μm and occur both as small inclusions within silicate phases or in larger forms at grain boundaries between all the major silicates. All sulphides occur as massive grains and no exsolution flames have been observed. Olivine crystals contain numerous tiny opaque inclusions (<2 μm) which lie along internal fracture surfaces within the crystals, these comprise the three igneous sulphide phases (Po, Pn, Cp) and at least one oxide phase (probably chromite given its early crystallisation), but their size precludes LA-ICP-MS analysis. Gabbroic eclogite sulphides are less numerous but typically much larger than those in gabbros (800 x 1000 μm in one case, Figure 1), suggesting recrystallisation in a hydrothermal or metamorphic fluid. The occurrence of transitional monoclinic/hexagonal pyrrhotite, together with pyrite and chalcopyrite, is inconsistent with low temperature (<250°C) equilibration (Kissin and Scott, 1982) and thus suggests formation during high-temperature hydrothermal alteration or HP metamorphism, with partial inversion to a monoclinic habit during cooling. Such an assemblage indicates relatively oxidising conditions, possibly in the presence of Fe-poor pyroxene (Harlov et al., 1997), a constituent of an eclogitic assemblage. The absence of either euhedral single-phase pyrite grains or sulphur gain in the gabbroic eclogites also strongly suggests a metamorphic origin for the eclogite sulphide assemblage (Luguet et al., 2004).

Metamorphic recrystallisation of basaltic sulphides has also resulted in the formation of pyrite at the expense of igneous sulphide phases. Pyrrhotite and pentlandite have not been identified in metabasalts but minor chalcopyrite remains (<10%). As there is no basaltic protolith preserved, the identity of initial sulphide phases is uncertain, but observations of other MORB (e.g. Czamanske and Moore, 1977; Roy-Barman et al., 1998) and the gabbros in this study suggest that an Fe-rich (monosulphide solid solution (mss) or pyrrhotite), Ni-rich (pentlandite) and Cu-rich sulphide (chalcopyrite or intermediate solid solution (iss)) would have been present. Chalcopyrite may have been present in greater proportion in the precursor

198 basalts than in the cumulate gabbros, given that MORB sulphide globules display positively
199 co-varying Ni/Cu and Mg number (Czamanske and Moore, 1977), presumably due to the
200 lower and higher solidi of Cu-rich and Fe-Ni-rich sulphide liquids, respectively. Unlike the
201 gabbroic samples, sulphides in basaltic eclogites display minor alteration to haematite
202 (<15%).

203 **2.3 Pressure-Temperature-time estimates for high-pressure metamorphism**

204 Pressure (P) – temperature (T) estimates for the equilibration of mineral assemblages in
205 gabbroic and basaltic eclogites have been obtained using the internally-consistent
206 thermodynamic dataset (THERMOCALC® program) of Holland & Powell (1985; 1990;
207 1998) and Powell & Holland (1985; 1988). As igneous compositional domains are retained in
208 some gabbroic eclogites, indicating disequilibrium, P-T estimates in these cases were
209 generated from individual domain assemblages and surrounding garnet coronas.

210 The peak metamorphic assemblage for gabbroic eclogites is typically garnet + omphacite +
211 paragonite + actinolite + clinozoisite + quartz ± chloritoid + fluid (CO_2-H_2O, x(H_2O) = 0.8).
212 Pressure estimates range from 1.9 to 2.2 GPa, while temperature varies between 500 and
213 580°C, similar to previous estimates for the Allalin Gabbro and Täschalp (Pfulwe) areas in
214 the northern ZSO (≥2.0 GPa and 550-600°C, Meyer, 1983; Barnicoat and Fry, 1986), but
215 lower than those for the Lago di Cignana area to the south (2.7-2.9 GPa and 600-630°C,
216 Reinecke, 1991). However, on the basis of carbonate phase equilibria, it has been suggested
217 that peak metamorphic pressures for the Allalin Gabbro may have reached 3.5 GPa
218 (Barnicoat, 1996). The assemblage in basaltic eclogites typically comprises garnet +
219 omphacite + muscovite + paragonite + glaucophane + clinozoisite + quartz + fluid (CO_2-H_2O,
220 x(H_2O) = 0.8). The P-T estimates for this assemblage are comparable to those for gabbroic
221 eclogites and vary between 1.9-2.2 GPa and 530-600°C, respectively. The significance of

such P-T conditions is that they are comparable to those typical of present-day subduction zones, where temperatures remain low for a given pressure.

Garnet Sm-Nd and metamorphic zircon U-Pb data yield ages for peak metamorphism of 40.6±2.6 Ma (Amato et al., 1999) and 44.1±0.7 Ma (Rubatto et al., 1998), respectively. A retrogressive greenschist facies age of 38±2 Ma (Rb-Sr) has been estimated, suggesting initially rapid exhumation (10-26 km/Ma, Amato et al., 1999) which evidently aided preservation of the high pressure assemblage with very little retrograde metamorphism.

2.4 Summary of published major and trace element chemistry

The major and trace element chemistry of the samples in this study has been previously described by Dale et al. (2007). Although the samples have been chemically altered by pervasive HP-LT metamorphism, the less 'fluid-mobile' elements such as the mid to heavy REE suggest an E-MORB-like initial composition for the basaltic eclogites (Dale et al., 2007). The chemistry of the gabbroic lithologies reflects their formation by crystal accumulation, particularly plagioclase (e.g. positive Sr, Ba and Eu anomalies). Whole-rock large-ion lithophile element (LILE: Ba, Rb, K) abundances have been depleted by up to 80% in both gabbroic and basaltic eclogites when compared to so-called 'fluid-immobile' elements such as Nb (Dale et al., 2007). Strontium is also depleted, particularly in the gabbroic eclogites, while there is apparently no loss of U from either gabbroic or basaltic material, possibly due to zircon growth during metamorphism.

3. ANALYTICAL TECHNIQUES (smaller type possible)

Whole-rocks. Whole rock powders (~1-2g;) were ground in agate, following crushing within plastic by hammer (to avoid steel contamination), and were digested and equilibrated with a mixed ^{190}Os–^{191}Ir–^{99}Ru–^{194}Pt–^{106}Pd-^{185}Re-enriched spike, using inverse aqua regia (2.5ml 12

mol l^{-1} HCl and 5ml 16 mol l^{-1} HNO_3) in quartz high-pressure asher (HPA) vessels. The vessels were placed in an Anton Paar HPA at Durham University at 300°C and 125 bars for at least 8 hours. The extraction and purification of Os, Ir, Ru, Pt, Pd and Re followed closely techniques described previously (Shirey and Walker, 1995; Cohen and Waters, 1996; Birck et al., 1997; Pearson and Woodland, 2000). Osmium was extracted from the inverse aqua regia using CCl_4, back-extracted using HBr, and then microdistilled. The aqua regia was dried and re-dissolved in 0.5 mol^{-1} HCl for purification of Re, Ir, Ru, Pt and Pd using AG1X-8 (100-200 mesh) anion-exchange resin.

Mineral separates. Mineral separates, hand-picked from gabbro and gabbroic eclogite samples, were optically inclusion-free, except olivine (which contains tiny opaque inclusions) and omphacite (contains exsolved rutile). The Re-Os data for olivine probably represent an upper concentration limit. Mineral separates of between 1.5 and 380 mg were cleaned in an ultrasonic bath using acetone, 2 mol l^{-1} HCl and water, dried and then powdered in agate. The procedure for dissolution and purification of Re and Os follows that of Birck et al. (1997), except that reduced volumes of reagents were used in order to minimise blanks.

Separated sulphides were processed at the Open University in either the same way as silicate separates or by microdistillation only. The latter technique involved the drying of ^{190}Os-^{185}Re-spike on the lid of a conical Teflon® vial, followed by placement of the sulphide, 25µl 12 mol l^{-1} H_2SO_4 and 20µl Cr in H_2SO_4 on the spike residue, and 15µl of 9 mol l^{-1} HBr in the apex of the vial. The vial was inverted and screwed tightly onto the lid and placed on a hotplate, resulting in full digestion, oxidation of Os and separation from Re (Pearson et al., 1998). Rhenium data for microdistilled sulphides are not presented due to considerable blank contribution.

Mass spectrometry. Whole-rock Re-Os and PGE analyses were performed at Durham University. Osmium was analysed on Pt filaments as OsO_3^- by negative-thermal ionisation mass spectrometry (N-TIMS) using the electron multiplier mode on a ThermoFinnigan Triton (after Creaser et al., 1991; Volkening et al., 1991). Repeat analyses (n=23) of 1.75 and 17 pg aliquots of the University of Maryland (College Park) Os reference material (UMd; also sometimes UMCP) at Durham University gave a $^{187}Os/^{188}Os$ mean value of 0.11378±28 (2 SD) over the time period of analysis (October 2005 – November 2007), in good agreement with a value of 0.113787±7 for much larger aliquots (>10 ng) measured on the same instrument in Faraday cup mode (Luguet et al., 2008a).

Whole-rock Re, Ir, Ru, Pt and Pd were measured by inductively-coupled plasma mass spectrometry (ICP-MS) on a ThermoFinnigan Element 2 at Durham University. Solutions were introduced using a MicroMist micro-concentric nebuliser and ESI stable sample introduction system (dual-cyclonic quartz spray chamber). Mixed solutions of natural PGE and solutions of Hf, Zr, Y and Mo (all at 1ng/g concentrations) were used to quantify the degree of mass fractionation and the production rates of HfO^+, ZrO^+, YO^+ and MoO^+ which are of equivalent mass to isotopes of Ir^+, Pt^+ and Pd^+. These solutions were analysed before, during and at the end of each analytical session.

Re-Os in mineral separates were analysed at the Open University. Osmium methodology followed that above, except for the use of the Johnson-Matthey (DTM) Os standard solution which gave a $^{187}Os/^{188}Os$ mean value of 0.17395±87 (2SD, n=18) for 0.5 and 1 pg aliquots, in good agreement with a value of 0.17394±1 for several ng Os, obtained by Birck et al. (1997). Rhenium was analysed by N-TIMS, as ReO_4^- ions.

290 *Blanks.* Total procedural blanks for Re-Os whole rock analyses (October 2005 to November
291 2007 were as follows (mean value in parentheses); Os: 0.04-0.51 pg (0.21) with $^{187}Os/^{188}Os$
292 between 0.140 and 0.675 (0.32), Ir: 0.05-1.1 pg (0.44), Ru: 0.5-4.2 pg (1.8), Pt: 1.9-5.6 pg
293 (3.4), Pd: 3-25 pg (10), Re: 0.3-9 pg (1.6). Although the absolute values for the blank varied
294 significantly due to reagent variability, the short-term reproducibility of the Os blank (relating
295 to each reagent batch) was usually ±10% or better, and therefore blank corrections relate to
296 the individual batch rather than the long-term mean. The percentage blank contribution to
297 each analysis was always <10% for Os (and typically <2%), <30% for Ir and Ru (typically
298 <10%), <15% for Pt (typically <5%), <38% for Pd (typically <10%) and <4% for Re
299 (typically <2%). Blanks for mineral separates and sulphides digested at the Open University
300 in 2004 were in the range: 0.01 - 0.36 pg Os and 0.7 - 1.6 pg Re and again, blank correction
301 was performed according to batch (blank contribution is shown in Table 4).

302 *Digestion efficacy, reproducibility and accuracy of HSE concentrations.* HPA digestion of
303 relatively silica-rich samples such as basalts is, as yet, not well documented. However, Re
304 and Os whole-rock data in this study replicate data obtained from an HF-HBr dissolution
305 (Dale et al., 2007), and illustrate that Re and Os concentrations are broadly comparable using
306 the two techniques. In order to further assess the efficacy of Re and PGE extraction from the
307 silicate matrix during HPA digestion, a desilicification test was undertaken on the basaltic
308 reference materials (RM) DR26 type 1 and TDB-1, and also 2 gabbros, 1 gabbroic eclogite
309 and 1 basaltic eclogite from this study. This involved initial dissolution in 6ml 29 mol l^{-1} HF
310 and 2ml 12 mol l^{-1} HCl, followed by a HPA aqua regia digestion. Although the dataset is
311 limited (Table 2), and thus susceptible to the effects of powder heterogeneity, it suggests that
312 Pt, Pd and Re may not be fully extracted from the whole-rock powder of the two basaltic
313 reference materials without an initial desilicification step (cf. Dale et al., 2008). However, the
314 desilicified gabbros, gabbroic eclogite and basaltic eclogite have concentrations of Re, Pt and

315 Pd in good agreement with non-desilicified digestions (between 80% and 125% in all cases).
316 Furthermore, the concentrations can be either higher, lower or essentially the same, suggesting
317 that powder heterogeneity is the significant factor, rather than differing digestion efficacy.

318 Overall, duplicate digestions of the same sample powder (Table 2, n=2-4) indicate
319 reproducibility better than 15% for Os, despite concentrations below 20 pg/g, 4-50% for Ir
320 (one sample contains <2 pg/g Ir), 4-61% for Ru, 10-30% for Pt, <15% for Pd and <25% for
321 Re (one analysis of S01/3iix omitted for Pt, Pd and Re), comparable to other low abundance
322 samples (cf. Pearson and Woodland, 2000).

323 The accuracy of whole-rock HSE concentrations is more difficult to evaluate, but the
324 reproducibility of data using two different digestion techniques suggests that incomplete
325 digestion and/or sample-spike equilibration is unlikely to be a significant consideration. Data
326 for the RM DR26 type 1 are broadly in agreement with published values (Table 2). The
327 replicates (n = 2) of EN026 are in good agreement with each other but give lower
328 concentrations for all PGE than published data. Meisel and Moser (2004) highlighted inter-
329 laboratory variation for this RM which requires further study; e.g. mean Ir concentrations vary
330 from 12 - 35 pg/g (Table 2). Data for standard HPA digestion (aqua regia, no HF) of TDB-1
331 lie within the range of Meisel and Moser (2004), while the desilicified analysis gave Ru, Pt,
332 Pd and Ru values above the range of uncertainty in that study (Table 2). In summary,
333 difficulties remain with heterogeneity in low PGE concentration RM and there is no clear
334 evidence that one digestion method is superior to others.

335 *In situ sulphide analysis.* Sulphide HSE concentrations were measured by laser-ablation ICP-
336 MS at the Open University, using a New Wave 213 Nd:YAG deep UV (213 nm) laser system
337 connected to an Agilent 7500s ICP-MS. Samples were prepared as 100-200μm thick polished

338 sections and the major element composition was established by electron microprobe (Cameca
339 SX100). Sulphur was used as an internal calibration for the ablation data. Ablation was
340 performed in a pure helium atmosphere, using a 40-80 μm beam size (depending on size of
341 sulphide) and a 10Hz laser frequency. The warm-up period was 150 seconds, the laser fired
342 for 50 seconds, and the wash-out duration between analyses was at least 320 seconds. The
343 data were processed in time-resolved mode using Glitter software (Van Achtebergh et al.
344 2001). Two 'in-house' external standards were used (initially synthesised at GEMOC,
345 Australia); the first, PGE-A, was used for calibrating all the PGE, and the second, ReOsOA#4,
346 was used for Re. Ruthenium masses 99 and 101 were both measured in order to assess
347 $^{61}Ni^{40}Ar^{+}$ and $^{59}Co^{40}Ar^{+}$interferences. A strong co-variation of ^{59}Co and ^{99}Ru, and the less
348 abundant ^{61}Ni and ^{101}Ru, was observed, suggesting significant argide interferences.
349 Concentrations given are derived from ^{101}Ru, because this isotope yielded lower
350 concentrations than ^{99}Ru, but the data for Ni-Co-rich sulphides could be significantly in error.
351 Rhodium concentrations in Cu-rich sulphides also suffer an interference from $^{63}Cu^{40}Ar^{+}$ on
352 $^{103}Rh^{+}$. A correction has been applied based on the $^{108}Pd/^{105}Pd$ ratio, which includes a
353 $^{65}Cu^{40}Ar$ interference on ^{105}Pd, but as the uncertainty increases with the size of correction,
354 some data have been omitted.

355 *Sulphur.* Whole-rock sulphur analyses were performed on a CS-125 LECO carbon and
356 sulphur determinator at the University of Leicester. Each sample (1g test portion) was
357 analysed three times, reproducibility was generally better than 4% (4 samples had poorer
358 reproducibility at 5-10%) and detection limits were typically 10 μg/g.

4. RESULTS

4.1 Whole-rock highly siderophile element (HSE) data

4.1.1 Gabbros and Gabbroic eclogites

Gabbros display chondrite-normalised PGE-Re patterns with high palladium group-PGE/iridium group-PGE ratios (Figure 2a) (PPGE: Pd,Pt,(Rh); IPGE: Os,Ir,Ru; Barnes et al., 1985). However, they possess slightly less fractionated PGE-Re patterns than MORB, with higher Os-Ir concentrations, comparable Pt and lower Re. Two gabbro groups are apparent on the basis of Pd content: one with high Pd_N/Pt_N (>1.25) and another with lower Pd_N/Pt_N (<1.25, Figure 2a). Transitional gabbros possess essentially the same PGE patterns as their precursor gabbros (Figure 2a) although two have lower Pd/Ir (and Pd/Pt). Gabbroic eclogites display strikingly variable chondrite-normalised PGE patterns (Figure 2b) which, for the most part, are fractionated with high PPGE/IPGE ratios (and high Re/IPGE), but Pt, Pd and possibly Ru concentrations appear to differ from the unaltered gabbros.

Figure 2 here.

All PGE concentrations in the gabbros vary by approximately two orders of magnitude (Table 2). Gabbroic Os concentrations display a larger range than gabbroic eclogites (2.3 to 321 pg/g and 1.6 to 105 pg/g, respectively), largely due to one PGE-rich gabbro. The ranges of Pt and Re are broadly comparable (Table 2), while the gabbro Ru range is somewhat larger (<10 to 581 pg/g) than the gabbroic eclogites (<6 to 95 pg/g). Palladium concentrations display the greatest difference, with gabbros varying from 13 to 1780 pg/g and gabbroic eclogites only from 19 to 176 pg/g.

The mean values for the gabbro and gabbroic eclogite suites are different (e.g. 64 and 31 pg/g Os respectively, Table 2). However, by omitting the one particularly PGE-rich gabbro, the

382 protoliths and their metamorphosed equivalents have indistinguishable mean concentrations:
383 Os - 27 and 31 pg/g, respectively, Ir - 19 and 24 pg/g, Ru - 41 and 41 pg/g and Pt - 243 and
384 243 pg/g (in each case 1 standard deviation is approximately equal to the mean itself). Mean
385 Re content differs slightly and is about 20% lower in the gabbros. Re-Os isotope data do not
386 permit significant loss or gain of Re or Os, unless shortly after igneous crystallisation (Dale et
387 al., 2007), and are therefore consistent with the similar mean concentrations derived from
388 omitting the PGE-rich gabbro. Given the low concentrations and heterogeneous distribution
389 of the PGE, coupled with an episode of metamorphism, the similarity in mean abundances is
390 remarkable.

391 In contrast to Pt, Re and the IPGE, mean Pd concentrations are markedly different in the
392 gabbroic and eclogitic suites (355 pg/g and 80 pg/g, respectively, Table 2 and Figure 2).
393 Assuming similar initial igneous concentrations of Pd, as with the other PGE, this equates to
394 Pd loss of ~75% (Figure 3). Lower Pd_{mean}/Ir_{mean} in the eclogites (3.4 compared to 18.4) and
395 typically lower Pd_N/Pt_N ratios (0.1 to 2.6 compared to 0.9 to 4.1), are also consistent with Pd
396 loss.

397 *MgO – PGE systematics.* Abundances of PGE and Re in the gabbros co-vary positively with
398 MgO content (e.g. Figure EA-1, electronic annex), with r^2 fits of 0.6 to 0.8. Chondrite-
399 normalised Os/Ir ratios (Os_N/Ir_N) for the gabbros range from 1.0 to 1.7, with a mean of 1.4,
400 and display no co-variation with MgO between 14 and 6.5 wt. % (Figure 4). Despite more
401 Os_N/Ir_N variability in the gabbroic eclogites, the mean of 1.3 is indistinguishable from the
402 gabbros. With one exception (namely the highest MgO sample) the gabbros define a positive
403 array between Ru_N/Ir_N and MgO, while gabbroic eclogites scatter to both higher and lower
404 ratios.

405 Figure 3 here.

406 Pt_N/Ir_N ratios in gabbros may increase and then decrease with decreasing MgO (Figure 4).
407 Gabbroic eclogites display considerable Pt_N/Ir_N variation for a given MgO content and have a
408 greater range of Pt_N/Ir_N ratios, extending both higher and lower than the gabbros (1.2 - 33.5
409 and 1.8 - 8.9, respectively). Gabbros with Pd_N/Pt_N >1.25 define a negative co-variation in
410 MgO - Pd_N/Ir_N space (r^2 – 0.97), whereas other gabbros plot below this array, towards a
411 cluster of gabbroic eclogites, which have significantly lower Pd_N/Ir_N.

412 Table 2 here.

413 Figure 4 here.

414 *4.1.2 Basaltic eclogites*

415 The variation in basaltic eclogite 'common' Os concentrations (after subtraction of in-grown
416 ^{187}Os) is fairly small, from 2.7 to 12 pg/g (Table 2), with a mean of 8.1 pg/g, similar to
417 MORB (~9 pg/g, Schiano et al., 1997; Escrig et al., 2004; Escrig et al., 2005; Gannoun et al.,
418 2007). Ruthenium concentrations (16 – 35 pg/g, mean: 26) are slightly lower than mean
419 MORB (47 pg/g, Rehkämper et al., 1999; Bezos et al., 2005).

420 The most striking aspect of basaltic eclogite PGE data is their extremely low Pd
421 concentrations relative to MORB (Table 2, Figures 4 and 5). The mean Pd concentration of
422 55 pg/g equates to a loss of ~90% when compared to ~660 pg/g for MORB (Rehkämper et al.,
423 1999; Bezos et al., 2005), and even accounting for substantial uncertainty in the MORB
424 average suggests loss of at least 85% (e.g. if MORB mean = 400 pg/g). Rhenium
425 concentrations are much lower than in MORB (398 pg/g and 1100 pg/g, respectively (Sun et
426 al., 2003; Gannoun et al., 2007)), suggesting ~60% loss, consistent with a previous study of
427 these rocks (Dale et al., 2007) and another study of metabasalts (Becker, 2000). The mean Pt
428 abundance of the metabasalts (112 pg/g) is also considerably lower than the MORB average

(~340 pg/g, Rehkämper et al., 1999; Bezos et al., 2005) despite one analysis with a fairly high Pt concentration (437 pg/g). The other basaltic eclogites have a mean Pt content of only 47 pg/g, and mostly have Pt/Ir ratios that are at the low end of the MORB range (Figure 4). Pt depletion in these rocks may be ≥60% on average, or ≥160 pg/g in actual terms, even when including the Pt-rich sample. Thus, basaltic eclogites have much flatter chondrite-normalised PGE patterns than typical MORB samples with significantly lower PPGE/IPGE (Figure 5).

Figure 5 here.

4.2 HSE abundances in gabbroic and eclogitic sulphides

Gabbro-hosted sulphides. Pyrrhotite displays relatively unfractionated PGE patterns with Pd_N/Ir_N of 0.2 to 6 (lowest in S01/36ix) and Re_N/Os_N of 1 to 9. However, Pt is fractionated from the other PGE and is present at exceptionally low normalised concentrations compared to Pd and Rh (Figure 6). This has previously been observed in mantle sulphides (Alard et al., 2000; Luguet et al., 2001; Lorand et al., 2008) where Pt is found to be concentrated in associated alloys, rather than being abundant in the sulphide itself. These Pt-rich alloys have been identified by discrete Pt spikes in the laser-ablation time-resolved spectrum in one of the gabbros analysed. Pentlandite also possesses low Pt concentrations, but has much higher Pd and somewhat higher Re, Rh and Ag (Figures 6 & 7 and Table 3). Chalcopyrite is enriched in Pd, Re, Ru, Ag and Pt, relative to pyrrhotite. Both pentlandite and chalcopyrite have slightly lower Os and Ir content than pyrrhotite and greater Re/Os ratios.

Figure 6 here.

Osmium concentrations in gabbro-hosted sulphides are heterogeneous and vary by up to 2 orders of magnitude, with a typical range of <0.003 to 0.07 µg/g (Table 3, mean: 0.043 µg/g). Rhenium concentrations are similarly heterogeneous and typically vary from 0.002 to 0.09

μg/g in all samples analysed (mean: ~0.014 μg/g). Almost all gabbro-hosted sulphides have Re/Os <1 (Figures 7 and 9), and mean Re/Os ratios are 0.29, 0.32 and 0.44 for the 3 different gabbros. Such Re concentrations and Re/Os ratios are considerably lower than the available data for MORB sulphides (0.069 to 3.2 μg/g and typically >1, Roy-Barman et al., 1998; Gannoun et al., 2004). Gabbroic sulphides have Pt abundances of <0.002 to 0.06 μg/g (Table 3), much lower than a published MORB sulphide (~30 μg/g, Peach et al., 1990), but as the latter was a bulk sulphide analysis (RNAA) it may have included associated Pt-rich micro-phases. Ruthenium tends to be significantly more abundant than Os and Ir, with a concentration range of at least <0.05 to 0.17 μg/g; argide interferences precluded accurate determination of Ru in pentlandite, but Ru has been shown to be compatible in this phase (Makovicky et al., 1985).

Palladium concentrations span nearly three orders of magnitude and, unlike the other PGE and Re, co-vary positively with sulphide Ni abundance (Figure 8), and to a lesser extent with Cu. This co-variation is particularly well-defined in two gabbros (r^2 = 0.83 and 0.98), which define two arrays with similar slopes but different absolute abundances, consistent with their different whole-rock Pd abundances. In contrast, eclogitic sulphides do not display co-variation of Pd and Ni and have a limited range of Ni content. Platinum does not co-vary with Ni in either gabbroic or eclogitic sulphides (Figure 8b), but it does display weak positive co-variation with Cu in some samples.

Table 3 here.

Figure 7 here.

Gabbroic eclogite-hosted sulphides. Unlike the sulphide assemblage in gabbros, pyrite is present and predominant in gabbroic eclogites, and pentlandite is absent. Pyrites from all

three eclogites have similar PGE-Re patterns and, compared to all gabbroic sulphide types, most have lower Os, Ru and Ir concentrations and very variable Pt contents (Figures 6 & 7 and Table 3). They also have higher Re concentrations and Re/Os ratios (0.04 to 69) than gabbroic sulphides (typically 0.04 to 4, e.g. Figure 10). All but one eclogite-hosted sulphide (Py, Po, Cp) has an Os/Ir ratio greater than unity. One gabbroic eclogite hosts a distinct pyrite group (group II in Figure 6) which has high Os-Ir concentrations, relatively high Pt, low Ru/Ir and very low Pd/Ir ratios. Cobalt contents of this group are higher than group I pyrites from the same sample, but within the range of all eclogitic pyrites analysed. Overall, the range of PGE concentrations in pyrites is broadly comparable to that of gabbroic sulphides, with the exception of Pd which is less concentrated in pyrite than in almost all gabbroic sulphides (Figure 7).

Figure 8 here.

4.3 Re-Os abundances in silicate and oxide mineral separates

4.3.1 Gabbroic minerals

Figure 9 illustrates broad co-variance of Re and Os in gabbroic silicates, oxides and sulphides. Plagioclase and the most inclusion-free olivine possess the most extreme Re/Os ratios observed in silicates and oxides (>350 and 3.7, respectively, Table 4). As expected for highly siderophile and chalcophile elements, Re and Os abundances in silicate phases are low and range from <0.5 pg/g in plagioclase, through augite (1-3 pg/g), and are highest in olivine (6-19 pg/g). A mixed ilmenite/chromite fraction contains ~130 pg/g Os, around ten times the whole-rock content.

Figure 9 here.

497 Rhenium concentrations in silicate and oxide phases are considerably higher than Os, perhaps
498 due to a different charge and ionic radius of Re in melts (cf. Ertel et al., 2001).
499 Concentrations in olivine range from 24 to ~710 pg/g in two separates from the same sample
500 (Table 4). Such a disparity is almost certainly due to the unavoidable sampling of Re-rich
501 inclusions, most likely sulphide but also probably chromite. Plagioclase and augite contain
502 Re at a concentration broadly comparable to the whole-rock (~170, ~120 and ~162 pg/g,
503 respectively). The Al-chromite + ilmenite fraction has relatively abundant Re (~1130 pg/g).

504 *4.3.2 Gabbroic eclogite minerals*

505 Os concentrations are less variable in eclogite phases (5 to 150 pg/g, Table 4) than gabbro
506 phases. Saussurite, the micro-crystalline multi-phase product of HP plagioclase breakdown,
507 possesses the lowest Os abundances, consistent with the low Os abundance of the precursor
508 phase. Coarse omphacite containing some rutile inclusions, likely formed in igneous
509 pyroxene domains, has Os concentrations of 13 and 33 pg/g in the two separates analysed.
510 Glaucophane and talc from the Os-rich eclogite S01/3iix both have surprisingly high Os
511 contents (90 and 150 pg/g, respectively) that may, in part, reflect inheritance of much of their
512 chemistry from the precursor olivine igneous domain containing numerous relatively Os-rich
513 sulphide and chromite inclusions.

514 Garnet contains by far the highest Re abundances (~1000 and ~7000 pg/g in two different
515 eclogites, Table 4). Saussurite, like its precursor plagioclase, contains ~75-140 pg/g Re.
516 Omphacite in one eclogite contains ~300 pg/g Re. Given that talc and glaucophane formed in
517 the same domain, it is evident that Re is preferentially incorporated into talc (600 and 350
518 pg/g) rather than glaucophane (~130 pg/g).

519 Table 4 here.

520

521 **4.4 Re-Os isotope data for minerals**

522 Whole-rock Re-Os data for Allalin gabbros and gabbroic eclogites presented in Dale et al.
523 (2007) give model ages and an errorchron age in broad agreement with the age of igneous
524 crystallization (164 Ma, Rubatto et al., 1998), demonstrating that the Re-Os system has not
525 been significantly disturbed during high-pressure metamorphism.

526 *Gabbros*. Whole-rock, olivine, augite and sulphide Re-Os measurements for S01/39iiix give
527 model ages which are close to the age of igneous crystallisation (Figure 10). This indicates
528 that even on a mineral-scale the Re-Os system remained largely 'closed' within
529 unrecrystallised samples, despite these rocks being subject to P-T conditions of 600°C and >2
530 GPa. However, an ilmenite and Al-chromite separate and a sulphide grain do yield young
531 model ages suggesting that the Re-Os system has locally been disturbed at the mineral scale
532 during metamorphism. Inclusion-rich olivine and augite from another gabbro (S02/83vix)
533 also have model ages broadly consistent with the age of igneous crystallisation (146 and 195
534 Ma, Figure 10).

535 Figure 10 here.

536 *Gabbroic eclogites*. By using an initial composition derived from the whole-rock at 45 Ma
537 ($^{187}Os/^{188}Os$ ~0.17), model ages close to the timing of peak metamorphism are generated
538 (Figure 10). The ages scatter considerably, but most of the phases measured yield ages within
539 uncertainty of the time of the peak of high-pressure metamorphism (ca. 45 Ma). These data
540 clearly indicate that the eclogitic minerals, both silicate and sulphide, relate to crystallisation
541 or equilibration at the time of HP metamorphism. In this case, the distribution of HSE must
542 also largely relate to the same HP metamorphism rather than some earlier event.

5. DISCUSSION

5.1 HSE systematics in whole-rock gabbros

In comparison with MORB, the relatively MgO-rich cumulate gabbros have less fractionated PGE patterns (lower PPGE/IPGE, Figure 2a). The IPGE are present in higher concentrations than in MORB, whereas Pt and Pd concentrations are similar and Re contents are lower. The relative compatibility of the PGE during fractional crystallisation in mid-ocean ridge systems, can be inferred by comparison of gabbro and MORB and is similar to that during mantle melting: i.e. Os≈Ir≥Ru>Pt>Pd>Re (e.g. Keays et al., 1981; Barnes et al., 1985). Thus, fractionation of the phases present in the cumulate gabbros (primarily olivine + plagioclase, but with associated sulphides and oxides) is likely to drive melts to increased PPGE/IPGE ratios. This observation can, in part, explain the generation of very high PPGE/IPGE ratios found in MORB (cf. Rehkämper et al., 1999; Tatsumi et al., 1999; Bezos et al., 2005), although significant fractionation of the PPGE and IPGE is still required during mantle melting.

The two gabbro groups, defined by Pd_N/Pt_N ratios (>1.25 and <1.25, Figure 2a), could be generated either by an igneous or post-igneous process. Magmatic variations in the modal proportion of different sulphide phases may account for such a difference, but the proportion of pyrrhotite, pentlandite and chalcopyrite does not seem to significantly vary between the groups. Furthermore, Pd_N/Ir_N variation is decoupled from differentiation indices such as MgO (Figure 4) and Ni, thus suggesting a post-igneous origin for the two groups. Gabbros with Pd_N/Pt_N >1.25 define a negative co-variation in MgO - Pd_N/Ir_N space ($r^2 = 0.97$), which likely represents the original magmatic array, whereas gabbros with Pd_N/Pt_N <1.25 plot below this array, towards the low Pd/Ir gabbroic eclogites, most likely due to minor Pd loss during alteration and/or metamorphism. Clearly the estimated degree of Pd loss between gabbroic

567 protolith and eclogite (>75%, Figure 3) depends on the origin of the Pd/Pt variation and if
568 some gabbros have experienced post-magmatic Pd loss then the true degree of loss from
569 pristine gabbro to gabbroic eclogite could be greater than estimated here.

570 There is clear positive co-variance between all the PGE (e.g. Figure EA-2). Os, Ir and Ru
571 display particularly well-defined arrays ($r^2 = 0.99$), but there is also positive co-variance of Os
572 with Pd and Pt ($r^2 = 0.63$ and 0.86, respectively). Rhenium-PGE co-variance is less clearly
573 defined, but is stronger with the PPGE than the IPGE. All whole-rock PGE abundances
574 decrease with decreasing MgO and sulphur content, in accord with extraction of immiscible
575 sulphide during fractional crystallisation due to sulphur-saturation of the magma (cf. Puchtel
576 and Humayun, 2000; Bezos et al., 2005), and the high sulphide-silicate melt partition
577 coefficients of the PGE (e.g. Peach et al., 1990). A comparison of PGE/Ir, Pd/Pt and Pt/Re
578 ratios with S content (not shown), suggests the relative order of PGE compatibility in the
579 gabbroic sulphides: Ir>Ru≈Os>Pd>Pt>Re (consistent with sulphide data in this study, except
580 Ir) or alternatively could suggest that sulphur content is driven by other changes in the
581 proportions of accumulating phases which instead control the PGE ratio variations. Similar
582 co-variation of PGE/Ir ratios and Cr abundance suggests that chromite could also play a
583 significant role in the fractionation of PGE through the nucleation of Os-Ir-Ru alloys, as
584 proposed by Ballhaus et al. (2006). However, the gabbroic whole-rock budgets of the IPGE
585 appear to be dominated by sulphide (section 4.5) and thus the variations reflect co-variation of
586 S and Cr, rather than control by chromite. Crystallisation of chromite would reduce FeO in
587 the melt, thus inducing sulphide precipitation (e.g. O'Neill and Mavrogenes, 2002).

588 Based on the slopes of the MgO-PGE/Ir arrays (Figure 4), and MgO-Pd/Pt, it can be inferred
589 that the relative bulk-rock PGE partition coefficients decrease in the following order:
590 Ru>Ir≈Os>Pt>Pd>Re. For instance, the positive array between Ru_N/Ir_N and MgO (6 to 14 wt.

591 %) in the gabbros suggests greater compatibility of Ru over Ir in the higher MgO
592 assemblages, which are also more S-rich (Table 2) due to greater sulphide precipitation
593 associated with olivine +/- chromite crystallisation. This order of relative bulk partitioning
594 differs slightly from that derived from PGE-sulphur systematics in that Ru appears to be the
595 most compatible on a bulk-rock scale. The greater bulk compatibility of Ru may be explained
596 by the positive co-variation of Ru/Os (and Ru/Ir) with modal proportion of olivine (Figure
597 EA-3), suggesting that Ru is more compatible (than Ir or Os) in this phase, although previous
598 experimental studies (Brenan et al., 2003; 2005) imply very similar olivine/melt partitioning
599 for Ru and Ir. Spinel and Fe-oxides, both present in the gabbros (Al-chromite and ilmenite),
600 have also been proposed as significant hosts of Ru (Capobianco and Drake, 1990; Capobianco
601 et al., 1994), but co-variation of Ru/Ir and the modal proportion of oxides is not observed in
602 these gabbros. Palladium is inferred to be more compatible than Pt in sulphide, but not in the
603 bulk-rock, consistent with Pt being hosted by other phases (Figure 12) and also reflecting the
604 extremely chalcophile nature of Pd (e.g. Peach et al., 1990).

605 It is possible that inflected, rather than straight, best-fit lines can be drawn through the MgO-
606 PGE/Ir data (Figure 4), although the inflection is largely based on one Mg-rich sample. Such
607 an inflection, if real, would indicate a change in bulk partitioning possibly due to a change in
608 the type of sulphide precipitated, or the cessation of chromite and/or associated PGE-rich
609 micro-phase crystallisation.

610 The inferred greater bulk compatibility of Ru over Ir in relatively Mg-rich samples (6 - 14 wt.
611 % MgO), is at odds with the observation that basalts, whose parental magmas have
612 presumably undergone significant fractional crystallisation of olivine, have higher chondrite-
613 normalised Ru contents than Os or Ir. However, this in part may be reconciled by the

614 generation of elevated Ru/Ir during partial melting and possibly by a change in partitioning
615 behaviour with MgO content, as suggested above.

616 Gabbroic Os_N/Ir_N ratios are greater than unity and are therefore higher than most mantle rocks
617 which contain roughly chondritic proportions of Os and Ir as a result of little fractionation
618 between these elements during mantle melting (Lorand et al., 1999; Pearson et al., 2004). The
619 chondritic Os/Ir ratio of the Mg-rich gabbro S02/6ix suggests that Os-Ir fractionation may
620 occur during early fractional crystallization (possibly due to sulphide precipitation or micro-
621 alloy formation), resulting in higher, and broadly constant, Os_N/Ir_N in lower MgO samples
622 (Figure 4).

623 **5.2 Whole-rock and mineral-scale HSE variations accompanying eclogite formation**

624 *5.2.1 Whole-rock HSE variations accompanying eclogitisation*

625 The mean abundances of the PGE in gabbros and gabbroic eclogites suggest that significant
626 fractional loss of Pd has occurred during metamorphism, equating to approximately 75% of
627 the original igneous concentration (or greater if some gabbros also record Pd loss). No other
628 PGE or Re appears to have been significantly depleted or enriched during metamorphism
629 (Figure 3). Mean concentrations of Re, Os and Ir are slightly higher in the gabbroic eclogite
630 suite than in the gabbros (if the anomalous PGE-rich gabbro, S02/6ix, is omitted). However,
631 these differences are not significant given the heterogeneous distribution of the PGE and the
632 relatively small sample set. Moreover, Re and Os are known, on the basis of isotope
633 evidence, not to have been significantly enriched or depleted in these samples during
634 metamorphism (Dale et al., 2007). Platinum has clearly been mobilised during
635 metamorphism (as illustrated by the highly variable Pt/Ir ratios of gabbroic eclogites), but the
636 degree of, or distance over which, this mobilisation has occurred was probably relatively

637 limited given that the mean Pt abundances of the gabbros and eclogites are essentially
638 identical.

639 In contrast, the basaltic eclogites display considerable depletion of Pt (≥60%), Pd (>85%) and
640 Re (50-60%, this study, Dale et al., 2007), relative to MORB (Figure 3). Rhenium loss of
641 ~60% has also been found in a study of other basaltic eclogites (Becker, 2000). The depletion
642 of Re is significantly less in percentage terms than that of Pd, but in absolute terms each
643 sample has lost, on average, ~600 pg/g Re, ≥350 pg/g Pd and ≥160 pg/g Pt. Some mobility of
644 Os, Ir or Ru cannot be ruled out as the means for basaltic eclogites are lower than mean
645 MORB (Os: -10%, Ir: -30%, Ru -45%), but at such low concentrations any estimate carries
646 considerable uncertainties.

647 As the temperature of metamorphism (~600°C) was insufficient to induce melting of hydrous
648 basalt or gabbro, it seems likely that Pd, Pt and Re were mobilised in a high-pressure fluid.
649 Gammons and Bloom (1993) and Wood et al. (1992) both found Pt and Pd to be soluble in
650 sulphur-bearing fluids, complexed with HS, although only the former concluded that Pd is
651 more soluble than Pt. The loss of Pd from both basaltic and gabbroic lithologies suggests that
652 this element is the most susceptible to release and mobility in a fluid. The observed loss of Pt
653 and Re from basaltic samples probably primarily results from a greater degree of hydration
654 and deformation than occurred in the gabbros. Deeply emplaced and massive gabbroic bodies
655 are likely to experience more limited hydrothermal and low-temperature seafloor alteration.
656 Thus, as a consequence of this limited alteration and their different rheological properties,
657 they will be less easily deformed during subduction.

658 *5.2.2 Distribution of HSE within a gabbro and a gabbroic eclogite*

659 Rhenium and Os concentrations in all the major constituent phases of a gabbro and a gabbroic
660 eclogite, combined from separated and in situ analyses (Tables 3 and 4), can be taken with the
661 estimated modal proportions of silicate and sulphide in order to calculate the contribution of
662 each phase to the whole rock budget of these elements. The in situ sulphide PGE data (Table
663 3) may also be combined with sulphur abundance to estimate the proportion of whole-rock
664 Os, Ir, Ru, Pt, Pd and Re accounted for by sulphide in the gabbros and gabbroic eclogites.

665 On the basis of electron probe micro-analysis (Table 1) and the sulphide phase modal
666 proportions, sulphide was taken to contain 36.5% S in the gabbroic samples and 47.5% S in
667 the eclogites. This was then combined with the sulphur concentration to calculate sulphide
668 abundance. It is important to note that calculated phase contributions to the Re and Os whole-
669 rock budget are poorly constrained due to uncertainties in estimating the modal proportions of
670 sulphide and silicate phases, the lack of replicate analyses of many phases, and limited laser-
671 ablation sampling of sulphide grains which have highly variable PGE abundances. Despite
672 such uncertainties, these data provide, for the first time, a quantitative estimate of the
673 proportion of HSE in silicate and sulphide phases from a gabbro and its metamorphosed
674 equivalent.

675 *Rhenium-osmium.* Approximately 90% of the whole rock abundance of Os in the gabbro
676 S01/39iiix can be accounted for by sulphide (Figure 11). Olivine and the oxide fraction
677 (chromite/ilmenite) together contain ~10% of the budget, but the olivine, while hand-picked,
678 unavoidably contained some sulphide and oxide inclusions so the percentage of Os in pure
679 olivine will almost certainly be lower still. By contrast, sulphide contains only ~5% of the
680 whole-rock Re. Plagioclase accounts for the majority of the Re budget (75-80%), while
681 augite contains <10% of the Re due to its much lower modal abundance. Oxides contain high

682 Re concentrations (1130 pg/g) but only account for a minor proportion of the whole-rock
683 (~5%) due to their low modal abundance.

684 Figure 11 here.

685 In the gabbroic eclogite S01/3iix, sulphide dominates the whole-rock budget of Os (~70%,
686 Figure 11). Glaucophane and talc, which crystallised within the olivine domain, account for
687 most of the remainder of the budget, probably due to inheritance of Os from the many tiny
688 sulphide inclusions originally within olivine. Garnet probably hosts the majority of Re, while
689 saussurite, the product of HP plagioclase breakdown, can also account for a significant
690 proportion.

691 *HSE in sulphides.* Gabbro-hosted sulphides (Po, Pn, Cp) account, on average, for >70% of
692 the whole-rock Os, Ir and Ru budget (Figure 12a). In two of the samples, sulphide
693 accommodates ~100% of the budget of these elements, whereas in the third, PGE-rich gabbro,
694 less than 30% of the IPGE can be accounted for by sulphide. The low proportion of PGE in
695 sulphides from this sample may be explained by the presence of tiny early-formed sulphide
696 inclusions in olivine, too small to be analysed, which are presumably PGE-rich compared to
697 later-precipitated inter-granular sulphides. Palladium is also largely hosted by sulphide,
698 particularly in the two PGE-poorer samples (~80%, mean: ~60%). The contribution of
699 sulphide to the whole-rock content of Pt and Re is very low; ~5% in both cases.

700 Despite large variations in the fraction of PGE accounted for by sulphide in the different
701 gabbroic eclogites, the mean percentage of whole-rock Os, Ir and Ru in gabbroic eclogite-
702 hosted sulphides (Py, Po, Cp) is significantly lower than in the gabbros (~50%, Figure 12b).
703 Platinum appears to be present in greater concentrations in the pyrite lattice than in gabbroic
704 sulphides (Figures 6 & 7), where it was probably concentrated in associated alloys, and hence

705 sulphide may account for as much as 30% of the eclogite whole-rock budget. Due to
706 considerably lower Pd concentrations, eclogitic sulphides can only account for about 40% of
707 the budget, despite much lower whole-rock Pd contents. The proportion of Re hosted by
708 sulphide is greater than in gabbroic sulphides but is still only ~15% of the whole-rock content.

709 Figure 12 here.

710 Basaltic sulphides, not included in this study, may possess different average PGE
711 concentrations to those in gabbros due to variation in sulphide type. With decreasing MgO
712 driven by fractional crystallisation, sulphide precipitation will change from predominantly
713 iron-rich to more copper-rich varieties (Czamanske and Moore, 1977). The latter are
714 preferred by the chalcophile Re and Pd (e.g. this study), resulting in higher Re/Os ratios in
715 MORB sulphides (cf. Gannoun et al., 2004). However, MORB sulphides still consist
716 primarily of mss/pyrrhotite, pentlandite and iss/chalcopyrite (Czamanske and Moore, 1977)
717 and hence it is reasonable to apply some of the findings from the gabbroic eclogites to the
718 interpretation of the basaltic eclogites.

719 *5.2.3 Mineral-scale evidence for the redistribution and loss of HSE during metamorphism*

720 The mean sulphur content of the gabbroic eclogites is 401 μg/g (n = 8), ~15-20% lower than
721 the gabbros (494 μg/g, n=8), perhaps suggesting a reduction in sulphur content between
722 igneous crystallisation and exhumation (although the data vary such that the two suites are
723 indistinguishable within uncertainty). Furthermore, there has been a predominant phase
724 change from igneous pyrrhotite + pentlandite (+ minor chalcopyrite) to more sulphur-rich
725 pyrite in the gabbroic eclogites (with subsidiary pyrrhotite and minor chalcopyrite). The
726 phase change marks coincident loss of nickel (and probably copper) from sulphide and
727 indicates evolution towards decreasing metal/S ratios in sulphide during metamorphism

728 (Table 1). Thus, the modal abundance of sulphide in the gabbroic eclogites has decreased by
729 a greater degree than S content from, on average, 0.135% in the gabbros to 0.084% in the
730 eclogites (38% reduction). The average sulphur content of the basaltic eclogites is ~1100
731 ug/g, which is within the range observed for MORB (1000 to 1800 Mathez, 1976). Thus, it is
732 not possible to ascertain whether the basalts have lost a significant proportion of sulphide, but
733 as with the gabbroic eclogites, sulphur appears to have been mobilised, modified and now
734 forms large grains predominantly composed of pyrite.

735 The whole-rock Pd budget is largely controlled by sulphide, and the highest Pd concentrations
736 are found in pentlandite (Figure 6, 7 & 8, section 4.2). Thus, the transformation from a
737 gabbroic sulphide assemblage of largely pyrrhotite + pentlandite to pyrite + pyrrhotite in
738 eclogites provides a mechanism for the release and loss of Pd from the whole-rock. In
739 contrast, Pt contents in eclogitic sulphides are typically higher than those in gabbros (Figure
740 7), and the proportion of whole-rock Pt hosted by eclogitic sulphides is greater (Figure 12).
741 This suggests that the Pt-rich micro-phases associated with the igneous sulphides may, at least
742 in part, have broken-down during metamorphism and, moreover, that much of this Pt has been
743 incorporated into the newly formed pyrite, rather than being mobilised on a larger scale.
744 Although no PGE data for basaltic eclogite sulphides are presented, the predominance of
745 pyrite and absence of Ni-rich sulphide, compared to sulphide globules in primitive MORB
746 glasses (Czamanske and Moore, 1977), is likely to account for much of the depletion of Pd.
747 However, in the case of the basalts, Pt is also clearly depleted. This difference in Pt mobility
748 could be due to greater deformation and fluid flow in the basalts, or possibly due to greater
749 retention of Pt in micro-phases in gabbros.

750 Transitional gabbros only display minor Pd depletion despite petrographical evidence for the
751 mobilisation of sulphide. However, there is little change in sulphide composition compared

752 to the gabbros (i.e. pyrrhotite > pentlandite > chalcopyrite). This is again consistent with the
753 majority of Pd loss being linked to changes in sulphide composition. Such evidence could be
754 taken as indicative of a difference in process (i.e. no Pd loss, therefore the loss is a result of
755 HP metamorphism) or a difference of degree (i.e. there is no Pd loss because the degree of
756 hydrothermal alteration was not as great as for the completely recrystallised eclogites). It is,
757 therefore, difficult to be certain that pyrite formation and loss of Pd is not the result of
758 hydrothermal activity. However, the absence of euhedral single phase pyrite crystals and the
759 fact that there is no increase in sulphur content in the gabbroic eclogites is strong evidence for
760 a metamorphic origin (Lorand and Juteau, 2000; Luguet et al., 2004). In any event, the Re-Os
761 model ages for sulphides (Figure 10) indicate recrystallisation or diffusional equilibration of
762 sulphide during HP metamorphism, probably with concurrent Pd loss.

763 The lack of whole-rock depletion of Os, Ir and Ru in gabbroic eclogites (Figure 3), despite
764 sulphides hosting a lower proportion of the whole-rock budget (Figure 12), requires Os, Ir and
765 Ru to be incorporated into silicate and/or alloy phases during metamorphism. The high Os
766 content of talc and glaucophane in the gabbroic eclogite S01/3iix (~90 and 150 pg/g,
767 respectively, Table 4) can largely account for the Os lost from sulphide. These concentrations
768 probably reflect inheritance from the precursor sulphide- and oxide-rich igneous olivine site,
769 rather than preferential partitioning into these phases. This inheritance suggests immobility of
770 Os in the fluid phase while the lack of whole-rock depletion also illustrates a lack of large-
771 scale mobilisation of Os, Ir or Ru. Whether Os is hosted in the lattice of amphibole or talc, or
772 whether they form tiny discrete PGE-rich micro-phases, cannot be determined.

773 The depletion of Re observed in the metabasalts (Figure 5) cannot be linked to the
774 transformation of sulphide mineralogy, due to the small contribution made by sulphides to the
775 whole-rock budget (Figures 11 & 12). Rhenium in gabbros is largely hosted in silicates

776 (plagioclase in particular). Although basaltic sulphides may contain greater abundances of Re
777 than those in gabbros (due to a greater proportion of Re-rich Cu-sulphides), the whole-rock
778 Re budget of basalts is also known to be largely hosted by silicates (Gannoun et al., 2004).
779 Despite evidence for strong Re partitioning into garnet in gabbroic eclogites (Figure 11, Table
780 4), this is clearly not a mechanism by which Re can be retained in basaltic crust, given the
781 apparent degree of Re depletion.

782 **5.3 Implications for recycling, sub-arc metasomatism and the source of super-**
783 **chondritic ^{187}Os and ^{186}Os compositions in OIB**

784 *Slab flux and sub-arc metasomatism.* The Re-Os isotope data of this and a previous study
785 indicate that the Re-Os system has remained 'closed' in ZSO gabbroic eclogites, and therefore
786 gabbro-derived fluids may not contain significant Re or Os (Dale et al., 2007). However, the
787 data from the basaltic portion of metamorphosed crust suggest a significant Re flux into the
788 sub-arc mantle (Figures 3 & 5). The Os elemental data for metabasalts are inconclusive,
789 although significant depletion seems unlikely. Some studies have concluded that Os is
790 transferred to the sub-arc mantle in significant quantities (e.g. Brandon et al., 1996; Borg et
791 al., 2000; Widom et al., 2003) while others have found no evidence of radiogenic Os transfer
792 (e.g. Chesley et al., 2002; Walker et al., 2002; Woodland et al., 2002). However, it has been
793 suggested that the mobility of Os in slab-derived fluids may depend on oxygen fugacity and
794 chlorine content (Brandon et al., 1996).

795 Subducting oceanic crust is likely to generate a significant flux of the PPGE into the sub-arc
796 mantle, with Pt derived from basaltic crust and Pd from both gabbroic and basaltic crust,
797 while the IPGE appear not to be significantly depleted in either metamorphosed gabbro or
798 basalt (Figure 13). Whether such a flux of Pt and Pd generates a noticeable enrichment in the
799 mantle perhaps depends on the degree of prior depletion of the mantle wedge (which would

reduce Pd and Pt concentrations) and also on fluid-rock ratios and whether there is a mechanism for further enrichment or concentration of the PGE in the fluid phase, perhaps through the stripping of PGE from peridotite. Regardless of the precise mechanism, high-degree enrichments of Pd and Pt, relative to the IPGE, have been previously identified in sub-arc mantle (McInnes et al., 1999; Kepezhinskas et al., 2002; Lee, 2002).

Figure 13 here.

The source of ^{187}Os-^{186}Os enrichment. The coupled enrichment of ^{187}Os (derived from ^{187}Re decay) and ^{186}Os (from decay of ^{190}Pt), found most notably in Hawaiian picrites, has been explained by a contribution from the outer core to mantle plume sources (Brandon et al., 1999; Puchtel et al., 2005), while others have suggested possible explanations via recycling of oceanic crust. Platinum abundances in the gabbros of this study are comparable to MORB (~360 and ~340 pg/g, respectively), although gabbros that have passed through subduction zones may retain higher concentrations of Pt than basalts, due to significant loss from the latter (>60%, this study). However, irrespective of whether Pt is lost from the subducting slab, Pt concentrations, and critically Pt/Re ratios, are not sufficiently high in basaltic or gabbroic crust to generate the most radiogenic $^{186}Os/^{188}Os$ ratios or the coupled ^{186}Os-^{187}Os enrichments found in OIB. Approximately 97% recycled oceanic crust contribution is required for the highest $^{186}Os/^{188}Os$ Hawaiian picrite, even if the crust was 2.5 Ga, while at these proportions $^{187}Os/^{188}Os$ would be much higher than observed (>1). Recently it has been proposed that coupled radiogenic $^{186}Os/^{188}Os$ and $^{187}Os/^{188}Os$ ratios in OIB could be generated by metasomatic sulphide in the mantle source, potentially emplaced by melt percolation derived from pyroxenite or peridotite (Luguet et al., 2008b). The loss of Pt and Re from basaltic crust (documented in this study) and their likely transfer into the mantle wedge by slab fluids, provides an alternative and globally widespread mechanism for the

824 generation of Pt- and Re-enriched material. Platinum concentrations in the oceanic crust are
825 low in comparison to mantle peridotite, but the large volume of continually subducting crust
826 could provide a major Pt flux. However, modelling of mantle enriched in this way suggests
827 that addition of slab-derived Re and Pt would not generate the observed ^{186}Os-^{187}Os
828 enrichments, due to low Pt/Re ratios. Thus, this mechanism would probably require further
829 scavenging of Pt from the overriding mantle wedge or the oceanic lithosphere, and/or
830 preferential enrichment of Pt in metasomatic sulphide.

831 ## 6. CONCLUDING REMARKS

832 The results presented here allow (i) quantification of the contribution of mineral phases to the
833 whole-rock PGE and Re abundances of gabbroic oceanic crust and the budget of the gabbroic
834 crust as a whole, and (ii) an assessment of the effects of subduction-related metamorphism on
835 whole-rock and mineral PGE abundances and distribution, and the implications for fluxes into
836 arc mantle and the PGE budget of recycled oceanic crust.

837 Gabbros possess chondrite-normalised PGE-Re patterns which are similar in shape and
838 concentration to mid-ocean ridge basalts, with high Pt-Pd-Re relative to Os-Ir-Ru. However,
839 they have slightly higher IPGE concentrations, consistent with their more primitive nature and
840 the relative compatibility of the PGE (Ir≈Os>Ru>Pt>Pd>Re).

841 Rhenium and Os abundances in gabbroic silicates, oxides and sulphides reveal that the Os
842 budget is almost entirely controlled by sulphide (particularly pyrrhotite). Rhenium, however,
843 is hosted mainly in silicates, particularly plagioclase (~75% in one sample) due to its
844 moderately high Re concentration (170 pg/g) and high modal abundance. Sulphide accounts
845 for <10% of whole-rock Re. Iridium, Ru and Pd are all predominantly hosted in sulphide
846 (typically >80% of the whole-rock budget), whereas chondrite-normalised Pt concentrations

847 are typically much lower than other PGE and only account for ~5% of the whole-rock budget.
848 Pt-rich micro-phases have been identified and probably significantly contribute to the budget.

849 Gabbroic eclogites, by comparison with their precursor gabbros, appear to be strongly
850 depleted in Pd (~75% loss). There is no evidence for significant loss of the other PGE or Re.
851 Platinum has been mobilised to a degree, as indicated by variable Pt/Ir ratios in gabbroic
852 eclogites, but the mean concentration is essentially identical to that of the gabbros. In
853 contrast, basaltic eclogites have significantly lower Pd, Pt and Re concentrations and lower
854 Pd-PGE/Ir-PGE ratios than mean MORB, suggesting losses of >85%, ≥60% and 50-60%,
855 respectively. The depletion of Pd in gabbroic and basaltic eclogites appears to be associated
856 with the loss of Pd-rich pentlandite probably during high-pressure metamorphism. Rhenium
857 and Pt depletion in the basalts, but not in the gabbros, is likely controlled by degree of
858 hydration, deformation and fluid flow, rather than directly by mineralogy. However, the
859 presence of Pt-rich micro-phases in gabbros provides a possible mechanism by which to
860 retain Pt. The compositional change of sulphide cannot account for Pt and Re depletion due
861 to the very small contribution that sulphide makes to the whole-rock budget of these elements.

862 Platinum abundances (~350 pg/g) and Pt/Re ratios in gabbros and basalts are not sufficiently
863 high, even if no Pt loss occurs, to generate the radiogenic $^{186}Os/^{188}Os$ ratios or the coupled
864 ^{186}Os-^{187}Os enrichments observed in some mantle-derived melts. However, Pt and Re loss
865 from the down-going slab provides a globally widespread mechanism for the formation of Pt-
866 and Re-rich metasomatised peridotite and/or metasomatic sulphides in the convecting mantle,
867 in a similar way to small degree melt interactions proposed by Luguet et al. (2008b).
868 However, due to the inferred low Pt/Re of slab-derived fluids, a subduction origin for ^{186}Os-
869 and ^{187}Os-enriched mantle material would require either a Pt/Re increase during fluid
870 transport or preferential enrichment of Pt over Re in metasomatic sulphide.

Acknowledgements.

The authors thank the Natural Environment Research Council (NERC) for supporting this work as part of C.D. PhD work, and as part of standard research grant (NE/C51902x/1). We are grateful to Tim Brewer and Sarah Lee for sulphur analyses, Chris Ottley for help with PGE and Re measurements and to Fatima Mokadem for assistance with laser ablation of sulphides. This manuscript was significantly improved following the comments of J.-P. Lorand, I. Puchtel and an anonymous reviewer. We thank M. Rehkamper for his editorial handling and comments.

Word Count:

main text was 13,372, then ~10930 (18% reduction), now 10416(~22% reduction)

abstract: 416

883 **References**

884 Alard, O., Griffin, W.L., Lorand, J.P., Jackson, S.E. and O'Reilly, S.Y., 2000. Non-chondritic
885 distribution of the highly siderophile elements in mantle sulphides. Nature, 407(6806):
886 891-894.

887 Amato, J.M., Johnson, C.M., Baumgartner, L.P. and Beard, B.L., 1999. Rapid exhumation of
888 the Zermatt-Saas ophiolite deduced from high-precision Sm-Nd and Rb-Sr
889 geochronology. Earth and Planetary Science Letters, 171(3): 425-438.

890 Anders, E. and Grevesse, N., 1989. Abundances of the Elements - Meteoritic and Solar.
891 Geochimica Et Cosmochimica Acta, 53(1): 197-214.

892 Ballhaus, C., Bockrath, C., Wohlgemuth-Ueberwasser, C., Laurenz, V. and Berndt, J., 2006.
893 Fractionation of the noble metals by physical processes. Contributions to Mineralogy
894 and Petrology, 152(6): 667-684.

895 Barnes, S.J., Naldrett, A.J. and Gorton, M.P., 1985. The Origin of the Fractionation of
896 Platinum-Group Elements in Terrestrial Magmas. Chemical Geology, 53(3-4): 303-
897 323.

898 Barnicoat, A.C. and Fry, N., 1986. High-Pressure Metamorphism of the Zermatt-Saas
899 Ophiolite Zone, Switzerland. Journal of the Geological Society, 143: 607-618.

900 Barnicoat, A.C., 1996. V71C-07: Dolomite breakdown under ultra-high pressure conditions in
901 the Allalin Gabbro of SW Switzerland. American Geophysical Union, 77: No. 762.

902 Barnicoat, A.C. and Cartwright, I., 1997. The gabbro-eclogite transformation: An oxygen
903 isotope and petrographic study of west Alpine ophiolites. Journal of Metamorphic
904 Geology, 15(1): 93-104.

905 Becker, H., 2000. Re-Os fractionation in eclogites and blueschists and the implications for
906 recycling of oceanic crust into the mantle. Earth and Planetary Science Letters, 177(3-
907 4): 287-300.

908 Bezos, A., Lorand, J.P., Humler, E. and Gros, M., 2005. Platinum-group element systematics
909 in Mid-Oceanic Ridge basaltic glasses from the Pacific, Atlantic, and Indian Oceans.
910 Geochimica et Cosmochimica Acta, 69(10): 2613-2627.

911 Birck, J.L., Barman, M.R. and Capmas, F., 1997. Re-Os isotopic measurements at the
912 femtomole level in natural samples. Geostandards Newsletter-the Journal of
913 Geostandards and Geoanalysis, 21(1): 19-27.

914 Bockrath, C., Ballhaus, C. and Holzheid, A., 2004. Fractionation of the platinum-group
915 elements during mantle melting. Science, 305(5692): 1951-1953.

916 Borg, L.E., Brandon, A.D., Clynne, M.A. and Walker, R.J., 2000. Re-Os isotopic systematics
917 of primitive lavas from the Lassen region of the Cascade arc, California. Earth and
918 Planetary Science Letters, 177(3-4): 301-317.

919 Borisov, A., Palme, H. and Spettel, B., 1994. Solubility of Palladium in Silicate Melts -
920 Implications for Core Formation in the Earth. Geochimica Et Cosmochimica Acta,
921 58(2): 705-716.

922 Brandon, A.D., Creaser, R.A., Shirey, S.B. and Carlson, R.W., 1996. Osmium recycling in
923 subduction zones. Science, 272(5263): 861-864.

924 Brandon, A.D., Norman, M.D., Walker, R.J. and Morgan, J.W., 1999. ^{186}Os-^{187}Os systematics
925 of Hawaiian picrites. Earth and Planetary Science Letters, 174(1-2): 25-42.

926 Brenan, J.M., McDonough, W.F. and Dalpe, C., 2003. Experimental constraints on the
927 partitioning of rhenium and some platinum-group elements between olivine and
928 silicate melt. Earth and Planetary Science Letters, 212(1-2): 135-150.

929 Brenan, J.M., McDonough, W.F. and Ash, R., 2005. An experimental study of the solubility
930 and partitioning of iridium, osmium and gold between olivine and silicate melt. Earth
931 and Planetary Science Letters, 237(3-4): 855-872.

932 Capobianco, C.J. and Drake, M.J., 1990. Partitioning of Ruthenium, Rhodium, and Palladium
933 between Spinel and Silicate Melt and Implications for Platinum Group Element
934 Fractionation Trends. Geochimica Et Cosmochimica Acta, 54(3): 869-874.

935 Capobianco, C.J., Hervig, R.L. and Drake, M.J., 1994. Experiments on Crystal Liquid
936 Partitioning of Ru, Rh and Pd for Magnetite and Hematite Solid-Solutions Crystallized
937 from Silicate Melt. Chemical Geology, 113(1-2): 23-43.

938 Chesley, J., Ruiz, J., Righter, K., Ferrari, L. and Gomez-Tuena, A., 2002. Source
939 contamination versus assimilation: an example from the Trans-Mexican Volcanic Arc.
940 Earth and Planetary Science Letters, 195(3-4): 211-221.

941 Chou, C.-L., 1978. Fractionation of siderophile elements in the Earth's upper mantle.
942 Proceedings of the Lunar Planetary Science Conference, IX: 219-230.

943 Cohen, A.S. and Waters, F.G., 1996. Separation of osmium from geological materials by
944 solvent extraction for analysis by thermal ionisation mass spectrometry. Analytica
945 Chimica Acta, 332(2-3): 269-275.

946 Creaser, R.A., Papanastassiou, D.A. and Wasserburg, G.J., 1991. Negative Thermal Ion
947 Mass-Spectrometry of Osmium, Rhenium, and Iridium. Geochimica Et Cosmochimica
948 Acta, 55(1): 397-401.

949 Czamanske, G.K. and Moore, J.G., 1977. Composition and Phase Chemistry of Sulfide
950 Globules in Basalt from Mid-Atlantic Ridge Rift Valley near 37degreesn Lat.
951 Geological Society of America Bulletin, 88(4): 587-599.

952 Dale, C.W., Gannoun, A., Burton, K.W., Argles, T.W. and Parkinson, I.J., 2007. Rhenium–
953 osmium isotope and elemental behaviour during subduction of oceanic crust and the
954 implications for mantle recycling. Earth and Planetary Science Letters, 253: 211-225.

955 Dale, C.W., Luguet, A., Macpherson, C.G., Pearson, D.G. and Hickey-Vargas, R., 2008.
956 Extreme platinum-group element fractionation and variable Os isotope compositions
957 in Philippine Sea Plate basalts: Tracing mantle source heterogeneity. Chemical
958 Geology, 248(3-4): 213-238.

959 Ertel, W., O'Neill, H.S., Sylvester, P.J. and Dingwell, D.B., 1999. Solubilities of Pt and Rh in
960 a haplobasaltic silicate melt at 1300 degrees C. Geochimica Et Cosmochimica Acta,
961 63(16): 2439-2449.

962 Ertel, W., O'Neill, H.S., Sylvester, P.J., Dingwell, D.B. and Spettel, B., 2001. The solubility
963 of rhenium in silicate melts: Implications for the geochemical properties of rhenium at
964 high temperatures. Geochimica et Cosmochimica Acta, 65(13): 2161-2170.

965 Escrig, S., Capmas, F., Dupre, B. and Allegre, C.J., 2004. Osmium isotopic constraints on the
966 nature of the DUPAL anomaly from Indian mid-ocean-ridge basalts. Nature,
967 431(7004): 59-63.

968 Escrig, S., Schiano, P., Schilling, J.G. and Allegre, C., 2005. Rhenium-osmium isotope
969 systematics in MORB from the Southern Mid-Atlantic Ridge (40 degrees-50 degrees
970 S). Earth and Planetary Science Letters, 235(3-4): 528-548.

971 Fleet, M.E., Crocket, J.H. and Stone, W.E., 1996. Partitioning of platinum-group elements
972 (Os, Ir, Ru, Pt, Pd) and gold between sulfide liquid and basalt melt. Geochimica Et
973 Cosmochimica Acta, 60(13): 2397-2412.

974 Gammons, C.H. and Bloom, M.S., 1993. Experimental Investigation of the Hydrothermal
975 Geochemistry of Platinum and Palladium .2. The Solubility of Pts and Pds in Aqueous
976 Sulfide Solutions to 300-Degrees-C. Geochimica Et Cosmochimica Acta, 57(11):
977 2451-2467.

978 Gannoun, A., Burton, K.W., Thomas, L.E., Parkinson, I.J., van Calsteren, P. and Schiano, P.,
979 2004. Osmium isotope heterogeneity in the constituent phases of mid- ocean ridge
980 basalts. Science, 303(5654): 70-72.

981 Gannoun, A., Burton, K.W., Parkinson, I.J., Alard, O., Schiano, P. and Thomas, L.E., 2007.
982 The scale and origin of the osmium isotope variations in mid-ocean ridge basalts.
983 Earth and Planetary Science Letters, 259(3-4): 541-556.

984 Harlov, D.E., Newton, R.C., Hansen, E.C. and Janardhan, A.S., 1997. Oxide and sulphide
985 minerals in highly oxidized, Rb-depleted, Archaean granulites of the Shevaroy Hills
986 Massif, South India: Oxidation states and the role of metamorphic fluids. Journal of
987 Metamorphic Geology, 15(6): 701-717.

988 Holland, T.J.B. and Powell, R., 1985. An Internally Consistent Thermodynamic Dataset with
989 Uncertainties and Correlations .2. Data and Results. Journal of Metamorphic Geology,
990 3(4): 343-370.

991 Holland, T.J.B. and Powell, R., 1990. An Enlarged and Updated Internally Consistent
992 Thermodynamic Dataset with Uncertainties and Correlations - the System K2o- Na2o-
993 Cao-Mgo-Mno-Feo-Fe2o3-Al2o3-Tio2-Sio2-C-H2-O2. Journal of Metamorphic
994 Geology, 8(1): 89-124.

995 Holland, T.J.B. and Powell, R., 1998. An internally consistent thermodynamic data set for
996 phases of petrological interest. Journal of Metamorphic Geology, 16(3): 309-343.

997 Holzheid, A., Sylvester, P., O'Neill, H.S.C., Rubie, D.C. and Palme, H., 2000. Evidence for a
998 late chondritic veneer in the Earth's mantle from high-pressure partitioning of
999 palladium and platinum. Nature, 406(6794): 396-399.

1000 Keays, R.R., Sewell, D.K.B. and Mitchell, R.H., 1981. Platinum and Palladium Minerals in
1001 Upper Mantle-Derived Iherzolites. Nature, 294(5842): 646-648.

1002 Kepezhinskas, P., Defant, M.J. and Widom, E., 2002. Abundance and distribution of PGE and
1003 Au in the island-arc mantle: implications for sub-arc metasomatism. Lithos, 60(3-4):
1004 113-128.

1005 Kissin, S.A. and Scott, S.D., 1982. Phase-Relations Involving Pyrrhotite Below 350-Degrees-
1006 C. Economic Geology, 77(7): 1739-1754.

1007 Lee, C.T.A., 2002. Platinum-group element geochemistry of peridotite xenoliths from the
1008 Sierra Nevada and the Basin and Range, California. Geochimica Et Cosmochimica
1009 Acta, 66(22): 3987-4005.

1010 Lorand, J.P., 1985. The Behavior of the Upper Mantle Sulfide Component during the
1011 Incipient Alteration of Alpine-Type Peridotites as Illustrated by the Beni-Bousera
1012 (Northern Morocco) and Ronda (Southern Spain) Ultramafic Bodies. Tschermaks
1013 Mineralogische Und Petrographische Mitteilungen, 34(3-4): 183-209.

1014 Lorand, J.P., Pattou, L. and Gros, M., 1999. Fractionation of platinum-group elements and
1015 gold in the upper mantle: a detailed study in Pyrenean orogenic lherzolites. Journal of
1016 Petrology, 40(6): 957-981.

1017 Lorand, J.P. and Juteau, T., 2000. The Haymiliyah Sulphide Ores (Haylayn Massif, Oman
1018 Ophiolite): In-situ segregation of PGE-poor magmatic sulphides in a fossil oceanic
1019 magma chamber. Marine Geophysical Researches, 21(3-4): 327-349.

1020 Lorand, J.P., Luguet, A., Alard, O., Bezos, A. and Meisel, T., 2008. Abundance and
1021 distribution of platinum-group elements in orogenic lherzolites; a case study in a
1022 Fontete Rouge lherzolite (French Pyrenees). Chemical Geology, 248(3-4): 174-194.

1023 Luguet, A., Alard, O., Lorand, J.P., Pearson, N.J., Ryan, C. and O'Reilly, S.Y., 2001. Laser-
1024 ablation microprobe (LAM)-ICPMS unravels the highly siderophile element
1025 geochemistry of the oceanic mantle. Earth and Planetary Science Letters, 189(3-4):
1026 285-294.

1027 Luguet, A., Lorand, J.P. and Seyler, M., 2003. Sulfide petrology and highly siderophile
1028 element geochemistry of abyssal peridotites: A coupled study of samples from the
1029 Kane Fracture Zone (45 degrees W 23 degrees 20N, MARK Area, Atlantic Ocean).
1030 Geochimica Et Cosmochimica Acta, 67(8): 1553-1570.

1031 Luguet, A., Lorand, J.-P., Alard, O. and Cottin, J.-Y., 2004. A multi-technique study of
1032 platinum group element systematic in some Ligurian ophiolitic peridotites, Italy.
1033 Chemical Geology, 208(1-4): 175-194.

1034 Luguet, A., Nowell, G.M. and Pearson, D.G., 2008a. $^{184}Os/^{188}Os$ and $^{186}Os/^{188}Os$
1035 measurements by Negative Thermal Ionisation Mass Spectrometry (N-TIMS): Effects
1036 of interfering element and mass fractionation corrections on data accuracy and
1037 precision. Chemical Geology, 248(3-4): 342-362.

1038 Luguet, A., Pearson, D.G., Nowell, G.M., Dreher, S.T., Coggon, J.A., Spetsius, Z.V. and
1039 Parman, S.W., 2008b. Enriched Pt-Re-Os isotope systematics in plume lavas
1040 explained by metasomatic sulfides. Science, 319(5862): 453-456.

1041 Makovicky, E., Makovicky, M. and Rosehansen, J., 1985. Experimental Studies on the
1042 Solubility and Distribution of Platinum-Group Elements in Base-Metal Sulfides in
1043 Platinum-Group-Mineral Deposits. Canadian Mineralogist, 23: 307-307.

1044 Mathez, E.A., 1976. Sulphur solubility and magmatic sulphides in submarine basalt glass.
1045 Journal of Geophysical Research, 81: 4249-4275.

McInnes, B.I.A., McBride, J.S., Evans, N.J., Lambert, D.D. and Andrew, A.S., 1999. Osmium isotope constraints on ore metal recycling in subduction zones. Science, 286(5439): 512-516.

Meisel, T. and Moser, J., 2004. Platinum-group element and rhenium concentrations in low abundance reference materials. Geostandards and Geoanalytical Research, 28(2): 233-250.

Meyer, J., 1983. The development of the high-pressure metamorphism in the Allalin metagabbro (Switzerland). Terra Cognita, 3: 187.

O'Neill, H.S.C. and Mavrogenes, J.A., 2002. The sulfide capacity and the sulfur content at sulfide saturation of silicate melts at 1400 degrees C and 1 bar. Journal of Petrology, 43(6): 1049-1087.

Peach, C.L., Mathez, E.A. and Keays, R.R., 1990. Sulfide Melt Silicate Melt Distribution Coefficients for Noble-Metals and Other Chalcophile Elements as Deduced from MORB - Implications for Partial Melting. Geochimica Et Cosmochimica Acta, 54(12): 3379-3389.

Pearson, D.G., Shirey, S.B., Harris, J.W. and Carlson, R.W., 1998. Sulphide inclusions in diamonds from the Koffiefontein kimberlite, S Africa: constraints on diamond ages and mantle Re-Os systematics. Earth and Planetary Science Letters, 160(3-4): 311-326.

Pearson, D.G. and Woodland, S.J., 2000. Solvent extraction/anion exchange separation and determination of PGEs (Os, Ir, Pt, Pd, Ru) and Re-Os isotopes in geological samples by isotope dilution ICP-MS. Chemical Geology, 165(1-2): 87-107.

Pearson, D.G., Irvine, G.J., Ionov, D.A., Boyd, F.R. and Dreibus, G.E., 2004. Re-Os isotope systematics and platinum group element fractionation during mantle melt extraction: a study of massif and xenolith peridotite suites. Chemical Geology, 208(1-4): 29-59.

Peregoedova, A., Barnes, S.J. and Baker, D.R., 2004. The formation of Pt-Ir alloys and Cu-Pd-rich sulfide melts by partial desulfurization of Fe-Ni-Cu sulfides: results of experiments and implications for natural systems. Chemical Geology, 208(1-4): 247-264.

1075 Peucker-Ehrenbrink, B., Bach, W., Hart, S.R., Blusztajn, J. and Abbruzzese, T., 2003.
1076 Rhenium-osmium isotope systematics and platinum group element concentrations in
1077 oceanic crust from DSDP/ODP sites 504 and 417/418. Geochemistry Geophysics
1078 Geosystems, 4(7): 10.1029/2002GC000414.

1079 Powell, R. and Holland, T.J.B., 1985. An Internally Consistent Thermodynamic Dataset with
1080 Uncertainties and Correlations .1. Methods and a Worked Example. Journal of
1081 Metamorphic Geology, 3(4): 327-342.

1082 Powell, R. and Holland, T.J.B., 1988. An Internally Consistent Dataset with Uncertainties and
1083 Correlations .3. Applications to Geobarometry, Worked Examples and a Computer-
1084 Program. Journal of Metamorphic Geology, 6(2): 173-204.

1085 Puchtel, I. and Humayun, M., 2000. Platinum group elements in Kostomuksha komatiites and
1086 basalts: Implications for oceanic crust recycling and core-mantle interaction.
1087 Geochimica Et Cosmochimica Acta, 64(24): 4227-4242.

1088 Puchtel, I.S., Brandon, A.D., Humayun, M. and Walker, R.J., 2005. Evidence for the early
1089 differentiation of the core from Pt-Re-Os isotope systematics of 2.8-Ga komatiites.
1090 Earth and Planetary Science Letters, 237(1-2): 118-134.

1091 Rehkämper, M., Halliday, A.N., Fitton, J.G., Lee, D.C., Wieneke, M. and Arndt, N.T., 1999.
1092 Ir, Ru, Pt, and Pd in basalts and komatiites: New constraints for the geochemical
1093 behavior of the platinum-group elements in the mantle. Geochimica et Cosmochimica
1094 Acta, 63(22): 3915-3934.

1095 Reinecke, T., 1991. Very-High-Pressure Metamorphism and Uplift of Coesite-bearing
1096 Metasediments from the Zermatt-Saas Zone, Western Alps. European Journal of
1097 Mineralogy, 3 (1): 7-17.

1098 Righter, K. and Drake, M.J., 1997. Metal-silicate equilibrium in a homogeneously accreting
1099 earth: New results for Re. Earth and Planetary Science Letters, 146(3-4): 541-553.

1100 Roy-Barman, M., Wasserburg, G.J., Papanastassiou, D.A. and Chaussidon, M., 1998.
1101 Osmium isotopic compositions and Re-Os concentrations in sulfide globules from
1102 basaltic glasses. Earth and Planetary Science Letters, 154(1-4): 331-347.

1103 Rubatto, D., Gebauer, D. and Fanning, M., 1998. Jurassic formation and Eocene subduction
1104 of the Zermatt-Saas- Fee ophiolites: implications for the geodynamic evolution of the
1105 Central and Western Alps. Contributions to Mineralogy and Petrology, 132(3): 269-
1106 287.

1107 Schiano, P., Birck, J.L. and Allegre, C.J., 1997. Osmium-strontium-neodymium-lead isotopic
1108 covariations in mid- ocean ridge basalt glasses and the heterogeneity of the upper
1109 mantle. Earth and Planetary Science Letters, 150(3-4): 363-379.

1110 Shirey, S.B. and Walker, R.J., 1995. Carius Tube Digestion for Low-Blank Rhenium-Osmium
1111 Analysis. Analytical Chemistry, 67(13): 2136-2141.

1112 Sun, W., Bennett, V.C., Eggins, S.M., Arculus, R.J. and Perfit, M.R., 2003. Rhenium
1113 systematics in submarine MORB and back-arc basin glasses: laser ablation ICP-MS
1114 results. Chemical Geology, 196(1-4): 259-281.

1115 Tatsumi, Y., Oguri, K. and Shimoda, G., 1999. The behaviour of platinum-group elements
1116 during magmatic differentiation in Hawaiian tholeiites. Geochemical Journal, 33(4):
1117 237-247.

1118 Van Achtebergh, E., Ryan, C. G., Jackson, S. E. and Griffin, W. L. (2001). Data reduction
1119 software for LA-ICP-MS. Laser-Ablation-ICPMS in the Earth Sciences: Principles and
1120 Applications, P. J. Sylvester (ed.). Mineral. Assoc. of Canada, Ottawa, Canada: 239-243.

1121 Volkening, J., Walczyk, T. and Heumann, K.G., 1991. Osmium Isotope Ratio Determinations
1122 by Negative Thermal Ionization Mass-Spectrometry. International Journal of Mass
1123 Spectrometry and Ion Processes, 105(2): 147-159.

1124 Walker, R.J., Prichard, H.M., Ishiwatari, A. and Pimentel, M., 2002. The osmium isotopic
1125 composition of convecting upper mantle deduced from ophiolite chromites.
1126 Geochimica et Cosmochimica Acta, 66(2): 329-345.

1127 Widom, E., Kepezhinskas, P. and Defant, M., 2003. The nature of metasomatism in the sub-
1128 arc mantle wedge: evidence from Re-Os isotopes in Kamchatka peridotite xenoliths.
1129 Chemical Geology, 196(1-4): 283-306.

1130 Wood, S.A., Mountain, B.W. and Pan, P., 1992. The Aqueous Geochemistry of Platinum,
1131 Palladium and Gold - Recent Experimental Constraints and a Reevaluation of
1132 Theoretical Predictions. Canadian Mineralogist, 30: 955-982.

1133 Woodland, S.J., Pearson, D.G. and Thirlwall, M.F., 2002. A platinum group element and Re-
1134 Os isotope investigation of siderophile element recycling in subduction zones:
1135 Comparison of Grenada, Lesser Antilles arc, and the Izu-Bonin arc. Journal of
1136 Petrology, 43(1): 171-198.
1137
1138

1139

1140 **FIGURE CAPTIONS**

1141 Figure 1. Composite sulphide grains from (a) gabbro S02/83vix and (b) gabbroic eclogite
1142 S01/40iiix. (a) Sulphide located between olivine and plagioclase. Pyrrhotite (Po) is the
1143 major gabbroic sulphide phase, but significant amounts of pentlandite (Pn) are also present.
1144 Chalcopyrite (Cp) is a minor constituent and usually forms at sulphide-silicate boundaries.
1145 The relative proportions of the three phases vary between grains, and also between samples.
1146 (b) Eclogitic sulphides have been recrystallised, are considerably larger and consist mainly of
1147 pyrite (Py), probably due to the addition of a sulphur-rich, iron-poor fluid, either during
1148 seafloor alteration or HP metamorphism. The grain pictured is unusual in the limited extent
1149 to which Py has formed. Note the absence of Pn and the retention of some Cp, although many
1150 eclogitic sulphides consist entirely of pyrite.

1151 Figure 2. Chondrite-normalised PGE-Re patterns for (a) gabbros, (b) gabbroic eclogites.
1152 Gabbros typically have smooth, fractionated PGE patterns with PPGE>IPGE, but less inter-
1153 element fractionation than the current MORB mean. Transitional gabbros are shown as light
1154 grey dashed lines in (a) and the corresponding gabbro is a black line with the same ornament.
1155 There is little variation (and no systematic variation) between transitional and preserved
1156 gabbros. Gabbroic eclogites display much greater variability and Pd concentrations are much
1157 lower than in the gabbros. CI chondrite values from Anders and Grevesse (1989).

1158 Figure 3. Relative mean difference in PGE and Re concentrations between gabbroic eclogite
1159 and precursor gabbro (darker shade, circles) and between basaltic eclogite and MORB (lighter
1160 shade, diamonds). Each mean is based on a small sample number (n=8) with a large range of
1161 PGE concentrations and so the standard deviation (SD) of each mean is approximately equal
1162 to the mean itself. Values used for MORB are, in pg/g: Os - 9, Ir* - 10, Ru - 47, Pt - 343, Pd -
1163 666 and Re - 1100 (Schiano et al. 1997; Rehkämper et al. 1999; Escrig et al. 2004, Bezos et

al. 2005; Escrig et al. 2005, Gannoun et al. 2007). * The current MORB mean for Ir is around 30 pg/g but given the mean for Os of <10pg/g from a greater number of samples, and their similar behaviour, a value of 10 pg/g Ir has been used.

Figure 4. Chondrite-normalised PGE/Ir variations with MgO for gabbros (dark field), gabbroic eclogites (G. eclogite, mid-shade field) and basaltic eclogites (B). Best-fit lines drawn by eye through the gabbro data. Os data are 'common Os' –calculated by subtraction of ingrown ^{187}Os. MORB data (light fields) from [1] Bezos et al. (2005) and [2] Rehkamper et al. (1999), CI chondrite values from Anders and Grevesse (1989).

Figure 5. PGE-Re patterns for ZSO basaltic eclogites. Thick dashed line is basaltic eclogite mean excluding high Pt sample. Basaltic eclogites contain significantly less Re, Pt and Pd than the MORB average estimate (details of which in Figure 3 caption). CI chondrite values: Anders and Grevesse (1989).

Figure 6. Chondrite-normalised PGE-Re patterns for laser-ablated sulphides from gabbros (a-b) and gabbroic eclogites (c-d). Symbol shapes denote host sample, colours denote sulphide type: Po – pyrrhotite, Pn – pentlandite, Cp – chalcopyrite, Py –pyrite. Legend ornaments are end-members, some analyses shown are composites indicated by combinations of colour. Small points indicate a large uncertainty due to interference or detection limit, and usually represent an upper limit. Dashed lines link such data+ to other data. (a) Igneous pyrrhotites are characterised by a small degree of fractionation except for Pt, which has low normalised concentrations; (b) & (d) Chalcopyrite and pentlandite have higher Pd/Ir and Re/Os ratios; (c) Pyrites in gabbroic eclogites display greater fractionation of the PGE, with much higher Re/Os ratios than igneous sulphides, and appear to define two groups, which we have termed I and II. CI chondrite values: Anders and Grevesse (1989).

1187 Figure 7. Pd vs. Os, Re and Pt for gabbro- and gabbroic eclogite-hosted sulphides (G and GE,
1188 respectively). Symbol colour and shape define sulphides from a single sample, ornament
1189 denotes sulphide type (commonly a composite analysis). Where present, dashed arrows
1190 indicate the plotted concentration is the detection limit, and the arrow indicates the direction
1191 of the 'true' concentration.

1192 Figure 8. Pd vs Ni and Pt vs Ni for sulphides from gabbros (G, squares) and gabbroic
1193 eclogites (GE, circles). Pd clearly co-varies positively with nickel in gabbroic sulphides (r^2 =
1194 0.98 for sample 83vix). There is little or no co-variation for eclogitic sulphides, which have
1195 lower Ni and Pd abundances and a smaller range of Ni content. Neither gabbroic nor
1196 eclogitic sulphides display co-variation between Ni and Pt. Small symbols signify Pd
1197 detection limit for analysis and are therefore only an upper constraint.

1198 Figure 9. Os vs. Re for individual silicate, oxide and sulphide mineral phases from two
1199 gabbros and two gabbroic eclogites. Sulphide data for S01/39iiix includes in situ data from
1200 S01/36ix which has comparable whole-rock PGE concentrations.

1201 Figure 10. Re-Os model age plotted against elemental Re/Os ratio for whole-rock and
1202 mineral analyses from two gabbros (S01/39iiix, black symbols; S02/83vix, blue) and one
1203 gabbroic eclogite (S01/3iix, light/unfilled symbols). Igneous mineral phases are typically
1204 close to, or within uncertainty of, the age of igneous crystallisation. Eclogitic mineral model
1205 ages have been calculated using the isotopic composition of the whole-rock at 45Ma (the
1206 timing of HP metamorphism, $^{187}Os/^{188}Os = 0.17$). Eclogitic phases have model ages which
1207 are consistent with mineral-scale resetting of the Re-Os system during HP metamorphism.
1208 Note the difference in Re/Os ratios observed in gabbroic and eclogitic sulphides.

Figure 11. Estimated contributions of constituent phases to the whole-rock Os and Re budget for a gabbro (S01/39iiix) and a gabbroic eclogite (S01/3iix), scaled to 100%. Due to limited sulphide Re data for S01/39iiix, in situ data from S01/36ix, which has a similar whole-rock Re concentration, has been incorporated.

Figure 12. Approximate average percentage of whole-rock PGE and Re hosted by sulphides in (a) gabbros (n=3) and (b) gabbroic eclogites (n=4). Given that sulphides in one particularly PGE-rich gabbro, S02/6ix, only account for <30% of the IPGE and <10% of the Pd, the typical proportion of IPGE and Pd hosted in gabbroic sulphides is likely to be closer to 100%.

Figure 13. Schematic cross section of a subduction zone illustrating probable elemental fluxes, and possible generation of Pt- and Re-enriched mantle that could form a source of coupled enrichments of ^{186}Os and ^{187}Os.

TABLES

Table 1. Major element compositions of typical sulphides from a gabbro and a gabbroic eclogite, determined by electron probe micro-analysis.

	Gabbro			Gabbroic eclogite		
	Po	**Pn**	**Cp**	**Py**	**Po**	**Cp**
S	38.38	32.48	34.81	53.18	39.27	34.99
Fe	61.30	40.51	30.82	46.55	59.47	30.71
Co	0.05	1.62	0.01	0.66	0.39	0.02
Ni	0.41	25.69	0.02	0.00	0.38	0.01
Zn	0.00	0.00	0.00	0.00	0.00	0.00
Cu	0.03	0.07	32.70	0.00	0.49	32.55
Cr	0.01	0.02	0.00	0.00	0.00	0.00
Tot	100.2	100.3	98.37	100.3	100.0	98.27
M/S	0.92	1.18	0.98	0.51	0.89	0.97

Notes: Po – pyrrhotite, Pn – pentlandite, Cp – chalcopyrite, Py – pyrite.

Composition and atomic metal/sulphur (M/S) ratios of pyrrhotites indicate a change in structure between gabbros and gabbroic eclogites, from hexagonal towards monoclinic (cf. Lorand and Juteau, 2000). In some cases, pyrrhotite in gabbros has been altered to troilite.

Table 2. PGE and Re concentrations and Re-Os isotopes in ZSO gabbros, gabbroic eclogites, transitional gabbros and basaltic eclogites

	Mass (g)	Os* ng/g	**Os** ng/g	**Ir** ng/g	**Ru** ng/g	**Pt** ng/g	**Pd** ng/g	**Re** ng/g	$^{187}Os/^{188}Os^{\alpha}$	$^{187}Re/^{188}Os$	**Model Age$^{\lambda}$**	**MgO** wt.%	**Ni** µg/g	**S** µg/g	**Yb** µg/g
Gabbros															
S01/5G	1.999	0.0104	0.0108	0.0074	0.021	0.131	0.096	0.202	0.3795 ± 0.0003	92.7	157	14.1	385	328	0.14
S01/36ix	1.000	0.0185	0.0189	0.013	0.031	0.232	0.122	0.189	0.2827 ± 0.0004	49.2	179	9.17	313	438	0.20
dupl [§§]	1.015	0.0196	0.0200	0.014	0.031	0.256	0.135	0.195	0.2770 ± 0.0005	47.9	177	-	-	-	-
S01/39iiix	1.065	0.0095	0.0097	0.0055	0.011	0.092	0.049	0.144	0.3114 ± 0.0002	73.5	143	10.3	386	311	0.18
S02/6ix	0.970	0.320	0.321	0.322	0.581	1.20	1.78	0.406	0.1502 ± 0.0001	6.11	149	17.7	546	1073	0.62
S02/10iiixG	1.016	0.063	0.063	0.047	0.081	0.590	1.37	0.102	0.1753 ± 0.0001	7.89	307	6.65	184	286	0.08
dupl.[§]	1.075	0.065	0.066	0.045	0.077	0.611	1.36	0.098	0.1756 ± 0.0001	7.25	339	-	-	-	-
dupl [§§]	1.018	-	-	0.045	0.069	0.519	1.45	0.087	0.1753 ± 0.0001	-	-	-	-	-	-
S02/83vix	1.031	0.075	0.075	0.056	0.125	0.559	0.716	0.290	0.1934 ± 0.0002	18.7	184	13.4	363	696	0.38
S02/83viix	1.503	0.0020	0.0023	0.0016	<0.010	0.019	0.013	0.179	1.180 ± 0.002	434	145	8.88	154	463	0.80
S02/83viiixG	1.006	0.0069	0.0071	0.0046	0.011	0.083	0.083	0.136	0.4109 ± 0.0005	94.5	174	10.7	349	355	0.19
		Mean	*0.064*	*0.057*	*0.108*	*0.363*	*0.532*	*0.206*							
		Mean[#]	*0.027*	*0.019*	*0.041*	*0.243*	*0.355*	*0.177*							
		Median	*0.015*	*0.011*	*0.026*	*0.187*	*0.112*	*0.185*							
Transitional															
S01/5E	1.057	0.0172	0.0178	0.011	0.025	0.134	0.068	0.401	0.4051 ± 0.0003	112	144	11.8	420	961	0.21
S02/10iiixE	1.159	0.038	0.039	0.026	0.050	0.566	0.979	0.203	0.2236 ± 0.0001	25.6	206	9.27	263	211	0.15
S02/83viiixE	1.025	0.0087	0.0089	0.0060	0.020	0.113	0.057	0.316	0.3634 ± 0.0003	176	77	11.1	369	407	0.18
		Mean	*0.022*	*0.014*	*0.031*	*0.271*	*0.368*	*0.307*							
Gabbroic eclogites															
S01/3iix	2.000	0.104	0.105	-	0.076	*12.8*	0.176	0.475	0.1767 ± 0.0001	22.1	133	7.80	172	549	0.37
dupl.[§]	1.022	0.098	0.098	0.073	0.083	0.937	0.073	0.131	0.1776 ± 0.0001	6.48	401	-	-	-	-
dupl [§]	1.082	0.099	0.099	0.079	0.075	0.835	0.082	0.124	0.1769 ± 0.0001	6.04	424	-	-	-	-
dupl [§§]	1.016	-	-	0.072	0.074	0.786	0.079	0.102	-	-	-	-	-	-	-
S01/35iix	1.035	0.045	0.045	0.039	0.089	0.095	0.103	0.221	0.2101 ± 0.0001	23.8	187	8.35	204	466	0.37
S01/35iiix	1.098	0.055	0.056	0.045	0.095	0.160	0.071	0.546	0.2431 ± 0.0001	47.6	135	7.03	124	920	0.78
S01/40iiix	1.010	0.0090	0.0092	0.0048	0.016	0.124	0.046	0.117	0.2755 ± 0.0001	62.7	133	12.3	385	167	0.13
S01/40vx	1.056	0.0192	0.0194	0.015	0.023	0.332	0.168	0.081	0.2001 ± 0.0001	20.4	189	11.9	292	146	0.23
S01/40viix	1.053	0.0115	0.0117	0.0071	-	0.124	0.123	0.068	0.2266 ± 0.0002	28.3	193	12.3	348	152	0.23
dupl.[§]	1.091	0.0128	0.0130	0.0069	0.018	0.150	0.111	0.067	0.2279 ± 0.0002	25.3	219	-	-	-	-
S02/84viix	1.759	0.0009	0.0016	0.0010	<0.006	0.013	0.019	0.387	6.081 ± 0.007	2076	172	8.84	156	555	1.23
S02/85ixE	0.908	0.0033	0.0035	0.0029	0.0069	0.199	0.0094	0.150	0.7523 ± 0.0008	222	167	6.80	149	255	0.66
		Mean	*0.031*	*0.024*	*0.041*	*0.243*	*0.080*	*0.227*							
		Median	*0.016*	*0.011*	*0.020*	*0.149*	*0.087*	*0.179*							
	Total gabbroic mean		*0.043*	*0.036*	*0.068*	*0.298*	*0.316*	*0.230*							
	Total gabbroic median		*0.018*	*0.011*	*0.023*	*0.137*	*0.096*	*0.202*							

	Mass (g)	Os* ng/g	Os ng/g	Ir ng/g	Ru ng/g	Pt ng/g	Pd ng/g	Re ng/g	$^{187}Os/^{188}Os^{\alpha}$	$^{187}Re/^{188}Os$	Model Age$^{\lambda}$	MgO wt.%	Ni µg/g	S µg/g	Yb µg/g
Basaltic eclogites															
S02/41ii	1.034	0.0039	0.0111	0.0034	0.016	0.027	0.065	0.606	14.30 ± 0.01	753	1120	5.20	46	1907	5.27
S02/41v	1.016	0.0027	0.0029	0.0011	0.016	0.041	0.091	0.120	0.7790 ± 0.0008	216	179	5.51	56	1210	4.87
dupl §§	1.034	-	-	0.0016	0.012	0.051	0.085	0.100	-	-	-	-	-	-	-
S02/74ii	1.092	0.0120	0.0132	0.0099	0.035	0.059	0.063	0.827	0.8634 ± 0.0006	332	131	6.17	113	1287	3.43
S02/75iiR	1.098	0.0120	0.0122	0.0078	0.021	0.437	0.050	0.062	0.2904 ± 0.0002	24.8	377	5.31	73	712	4.31
S02/75iiiC	1.012	0.0088	0.0096	0.011	0.034	0.057	0.029	0.237	0.8344 ± 0.0005	130	323	5.63	72	932	4.92
S02/75iiiR	1.022	0.0095	0.0103	0.0096	0.034	0.048	0.038	0.540	0.7441 ± 0.0005	274	133	6.46	91	538	3.82
	Mean	*0.008*	*0.010*	*0.007*	*0.026*	*0.112*	*0.055*	*0.397*							
	Median	*0.009*	*0.011*	*0.009*	*0.028*	*0.052*	*0.056*	*0.389*							
Reference materials															
DR26 type 1	*1.003*		*0.014*	*0.007*	*-*	*0.359*	*1.26*	*0.443*	*0.2386 ± 0.0002*	*149*	*44*				
dupl §§	*1.005*		*0.020*	*0.015*	*0.081*	*0.673*	*1.49*	*0.534*	*0.2640 ± 0.0002*	*128*	*64*				
dupl §§	*1.006*		*0.015*	*0.012*	*0.073*	*0.421*	*1.44*	*0.506*	*0.2228 ± 0.0002*	*160*	*35*				
Paris mean			*-*	*0.054±0.095*	*0.064±0.022*	*0.64±0.37*	*1.38±0.15*	*-*							
EN026 10D-3	*1.005*		*0.010*	*0.012*	*0.031*	*0.286*	*0.670*	*0.483*	*0.1697 ± 0.0029*	*233*	*11*				
dupl §	*1.997*		*0.008*	*0.011*	*0.030*	*0.218*	*0.690*	*0.470*	*0.1585 ± 0.0018*	*284*	*6.3*				
MUL mean			*0.018±0.054*	*0.036±0.034*	*0.041±0.007*	*0.37±0.12*	*0.72±0.09*	*0.516±0.057*	*0.137 ± 0.008*						
WHOI mean			*0.017±0.013*	*0.027±0.014*	*-*	*0.60±0.46*	*1.47±0.25*	*-*	*0.160±0.013*						
URI mean			*-*	*0.019±0.012*	*0.047±0.010*	*0.84±0.14*	*1.75±0.39*	*1.38±0.52*							
TDB-1	1.010		0.104	0.059	0.191	4.63	24.7	0.809	0.9688 ± 0.0003	41.5	1214				
dupl §§	1.011		-	0.061	0.256	5.82	34	0.978	0.9077 ± 0.0003	-	-				
MUL mean			*0.117±0.028*	*0.075±0.023*	*0.198±0.020*	*5.01±0.45*	*24.3±4.6*	*0.794±0.057*	*0.92 ± 0.20*	*35.9±10.1*	*1322±90*				
WHOI mean			*0.122±0.016*	*0.078±0.014*	*-*	*4.40±0.66*	*24.8±2.5*	*-*	*-*						

Notes:

Comprehensive major and trace element data available in the supplementary online material of Dale et al. (2007).

Significant figures: In order to permit accurate use of the data (e.g. low concentration Os/Ir ratios, which are readily reproducible) concentrations of some samples are quoted to 4 significant figures; such precision is reasonable for individual dissolutions. However, duplicate digestions demonstrate that the overall uncertainty for sample concentration, discussed in the text, is considerably greater.

Os* is the Os concentration after subtraction of ingrown ^{187}Os

Mean#: This is the average gabbro composition, omitting sample S02/6ix, which has anomalously high PGE concentrations. Omission, which gives similar means for gabbros and gabbroic eclogites, is justified by Os isotope data that demonstrate no significant change of Os concentrations by metamorphism.

$^{\alpha}$ Isotope ratios are blank corrected. Uncertainties are 2σ mean; $^{187}Os/^{188}Os$ ratios normalised using $^{192}Os/^{188}Os$=3.08271 & corrected using $^{18}O/^{16}O$ and $^{17}O/^{16}O$ of 0.002045 and 0.000371 respectively.

$^{\lambda}$ Model ages were calculated using $TMa=1/\lambda*Ln[(^{187}Os/^{188}Os_{isochron}-^{187}Os/^{188}Os_{sample})/(^{187}Re/^{188}Os_{chond}-^{187}Re/^{188}Os_{sample})+1]/1000000$, where $^{187}Os/^{188}Os_{isochron}$ is the initial (0.137) of the errochron defined by these samples in Dale et al. (2007).

The Pt concentration in grey italics is thought to be due to the so-called 'nugget effect', which can affect small sample mass digestions, and is probably unrepresentative.

§ Replicate analyses of the same powder, through repeated chemistry.

§§ Replicate analyses of the same powder, through repeated chemistry, including an initial HF-HCl desilicification step.

Reference material data in italics previously published in Dale et al., (2008). Published means and uncertainties for reference materials (also in italics, Paris – IPGP / MNHN, Bezos et al. (2005); MUL – Mulhouse and URI – University of Rhode Island, Meisel and Moser (2004) and ref. therein; WHOI – Woods Hole Oceanographic Institution, Peucker-Ehrenbrink et al. (2003).

Table 3. HSE concentrations (µg/g) and estimated contribution of each sulphide end-member for laser-ablation ICP-MS analyses of gabbro- and gabbroic eclogite hosted sulphides. Po – pyrrhotite, Pn – pentlandite, Cp – chalcopyrite, Py – pyrite. Ru and Rh data in grey italics carry greater uncertainties due to argide interferences. For other data, where '<' is used, the value quoted is defined by the detection limit.

	S01/36ix (G)							***S02/6ix (G)***						
	Po	**Po**	**Po**	**Po(Pn)**	**Pn/Po**	**Po/Cp(Pn)**	**Cp/Po/Py**	**Po**	**Po**	**Po**	**Po**	**Po/Pn(Cp)**	**Pn(Po)**	**Pn/Cp(Po)**
% Po	100	97	94	89	51	54	37	100	99	99	98	72	21	20
% Pn	-	3	3	10	49	12	21	-	1	-	1	13	76	57
% Cp	-	1	3	1	0	35	41	-	1	1	-	15	3	23
Os	0.050	0.047	0.045	0.034	0.027	0.032	0.017	0.018	0.018	<0.011	0.059	0.053	<0.013	0.048
Ir	0.034	0.039	0.018	0.019	0.014	0.017	<0.003	0.009	0.006	0.019	0.014	0.024	0.023	0.018
Ru *	*<0.142*	*<0.081*	*<0.243*	0.049	*<0.090*	0.067	0.033	0.016	0.023	<0.051	0.073	*<0.125*	*<0.411*	*<0.160*
Rh **	0.001	*<0.032*	-	*<0.06*	<0.003	*0.072*	*0.129*	<0.001	*0.006*	0.036	0.014	-	-	-
Pt	0.006	0.003	<0.002	<0.003	<0.004	<0.003	0.009	<0.002	<0.002	<0.016	<0.009	<0.007	<0.017	0.090
Pd	0.015	0.026	<0.005	0.072	0.192	0.092	0.169	0.017	0.021	0.090	0.035	0.364	0.226	<0.083
Re	0.006	0.011	0.002	0.006	0.009	0.076	0.003	0.003	0.002	<0.008	<0.004	0.010	0.015	0.042
Au	<0.002	<0.002	<0.002	<0.002	<0.003	<0.002	0.004	<0.002	<0.002	<0.010	<0.006	0.025	<0.012	<0.022
Ag	0.232	0.377	0.446	0.571	0.121	2.85	2.05	0.106	0.048	0.404	0.372	0.83	0.561	1.20

	S02/83vix (G)												***S02/84viix (GE)***		
	Po	**Po**	**Po(Cp)**	**Po(Pn)**	**Po(PnC**	**Po/Pn**	**Pn/Po**	**Pn**	**Pn(Cp)**	**Cp/Pn**	**Cp**	**Po/Cp**	**Py**	**Py**	**Py**
% Py	-	-	-	-	-	-	-	-	-	-	-	-	98	100	100
% Po	99	95	91	88	85	55	39		-			70	-	-	-
% Pn	1	2	1	12	8	39	58	105	90	45	4	8	-	-	-
% Cp	-	3	8	1	7	6	3	2	10	57	105	22	2	-	-
Os	0.028	0.011	0.028	0.067	0.126	<0.004	<0.003	0.023	<0.004	<0.005	<0.021	0.321	0.002	0.003	0.002
Ir	0.014	0.010	0.015	0.015	0.080	0.004	<0.002	0.016	0.004	0.005	<0.013	0.140	0.002	0.002	0.001
Ru *	0.034	0.042	0.033	*<0.050*	*<0.204*	*<0.178*	*<0.301*	*<0.495*	*<0.524*	*<0.275*	0.171	*<0.220*	<0.005	<0.012	<0.008
Rh **	0.002	*0.028*	*0.012*	0.027	*0.050*	-	*<0.21*	*0.027*	*0.008*	-	-	-	-	0.007	0.004
Pt	0.003	0.004	0.007	0.022	0.017	<0.005	0.006	<0.002	0.010	0.017	0.058	0.057	0.006	0.023	0.008
Pd	0.030	0.067	0.049	0.253	0.150	0.886	1.266	1.982	1.453	0.783	0.102	0.224	0.032	<0.009	<0.007
Re	0.003	0.006	0.010	0.011	0.010	0.090	0.003	0.003	0.004	0.011	<0.013	0.022	0.131	0.073	0.127
Au	<0.002	0.009	<0.002	0.002	0.014	0.011	<0.003	0.003	<0.003	0.005	<0.019	0.003	0.038	<0.003	<0.002
Ag	0.915	2.39	1.14	5.63	3.40	3.90	4.33	2.97	16.3	9.65	3.05	5.91	1.24	0.779	0.077

	S01/3iix (GE)						***S01/40iiix (GE)***					***S02/85ixE (GE)***			
	Py	**Py**	**Py**	**Py**	**Py**	**Po/Cp**	**Py**	**Py**	**Po**	**Po/Cp**	**Cp/Py**	**Py**	**Py**	**Py**	**Po(Cp)**
% Py	100	99	100	96	100		99	99		67	45	99	100	100	-
% Po	-	-	-	-	-	78	-	-	98	-	-	-	-	-	87
% Pn	-	-	-	-	-	1	1	1	2	5	1	1	-	-	1
% Cp	-	1	-	3	-	22	-	-	-	27	54	-	-	-	12
Os	0.004	0.015	0.072	0.112	0.204	0.007	0.002	0.001	0.001	0.002	0.005	0.001	0.003	0.001	0.004
Ir	0.001	0.004	0.046	0.137	0.192	0.003	0.001	0.001	0.001	0.001	0.002	0.001	0.003	0.001	0.002
Ru *	0.003	0.004	0.021	0.042	0.070	0.022	0.008	<0.006	0.012	*<0.031*	0.045	<0.003	0.004	<0.005	<0.010
Rh **	0.001	*<0.058*	<0.014	*0.015*	0.022	-	0.002	<0.009	*<0.019*	-	-	<0.001	0.002	<0.001	-
Pt	0.043	0.062	0.170	0.167	0.125	0.025	0.004	0.009	0.002	0.026	0.081	<0.001	<0.001	0.002	<0.003
Pd	0.009	0.015	0.007	0.013	0.012	0.322	0.012	<0.004	0.014	0.054	0.098	<0.002	0.005	0.005	0.039
Re	0.041	0.005	0.021	0.009	0.009	0.004	0.007	0.011	0.031	0.022	0.052	0.002	0.002	0.019	0.033
Au	0.001	0.020	0.001	<0.003	<0.004	0.039	<0.001	<0.002	<0.001	<0.002	0.003	0.001	0.001	<0.001	0.044
Ag	0.062	0.217	0.680	3.62	0.028	2.21	0.033	0.071	0.140	2.31	2.83	0.024	0.031	0.121	3.83

Table 4. Re-Os abundances and isotope data for separated silicate and sulphide phases from two gabbros and two eclogites. Data obtained by isotope-dilution N-TIMS.

	Mass (mg)	Re (ng/g)	Os (ng/g)	Os* (ng/g)	$^{187}Os/^{188}Os$	$^{187}Re/^{188}Os$	Blank (%)‡ Os	Blank (%)‡ Re	Model age[a]	Model age[b]	Prop. W.R.(%)# Os	Prop. W.R.(%)# Re
Gabbros												
S01/39iiix												
Whole rock	*460.1*	*0.139*	*0.011*	*0.011*	*0.3336 ± 0.0042*	*61.3 ± 3*	*7*	*19*	*194*	-	-	-
dupl.	*406.6*	*0.204*	*0.020*	*0.020*	*0.3005 ± 0.0028*	*50.4 ± 1*	*1*	*5.4*	*196*	-	-	-
dupl.§	1061	0.144	0.010	0.009	0.3114 ± 0.0002	74 ± 2	1	1	143	-	-	-
Silicates												
Olivine	380.8	0.024	0.0067	0.0066	0.217 ± 0.007	17.3 ± 0.5	2	12	285	-	9	3
Olivine	2.00	0.71	0.045	0.044	0.275 ± 0.021	79 ± 21	12	60	105	-	59	164
Olivine	45.39	0.35	0.024	0.024	-	71 ± 9	5	7	-	-	31	42
Plagioclase	64.75	0.17	<0.0005	-	-	~4000	80	10	-	-	1	67
Augite	44.26	0.12	0.001	0.001	1.414 ± 0.174	510 ± 100	47	19	150	-	1	8
Oxides												
Opaques (Ilmenite & Al-chromite)	1.83	1.13	0.128	0.127	0.167 ± 0.006	43 ± 9	5	55	45	-	4	5
Sulphides	(µg)											
Sulphide[m]	27.30	-	9.3	8.7	0.678 ± 0.012	-	4		-	-	50	*341*
Sulphide[m]	9.00	-	19.1	18.5	0.340 ± 0.010	-	6	-	-	-	103	-
Sulphide	15460	37.4	36.7	36.6	0.144 ± 0.000	4.9 ± 0.1	0	0.2	119	-	198	*18*
S01/83vix												
Whole rock	*411.0*	*0.288*	*0.081*	*0.081*	*0.1926 ± 0.0008*	*17.2 ± 0.2*	*1*	*11.6*	*199*	-	-	-
dupl.	*2093*	*0.313*	*0.079*	*0.078*	*0.1941 ± 0.0001*	*19.3 ± 0.3*	*0*	*1.4*	*181*	-	-	-
dupl.	*305.4*	*0.276*	*0.079*	*0.078*	*0.1935 ± 0.0006*	*16.9 ± 0.3*	*0*	*11*	*205*	-	-	-
dupl.§	1031	0.290	0.075	0.075	0.1934 ± 0.0002	18.7 ± 0.2	0	11	184	-	-	-
Silicates												
Olivine	10.36	0.42	0.019	0.019	0.184 ± 0.006	109 ± 11	6	33	26	-	-	-
Augite	24.34	0.048	0.003	0.003	0.411 ± 0.041	85 ± 38	16	65	195	-	-	-
Olivine (many opaque inclusions)	1.52	0.78	0.36	0.36	0.161 ± 0.015	12 ± 3	2	48	134	-	-	-
Gabbroic eclogites												
S01/3iix												
Whole rock	*419.9*	*0.220*	*0.048*	*0.047*	*0.1944 ± 0.0013*	*22.4 ± 0.3*	*0*	*4*	*157*	-	-	-
dupl.	*398.2*	*0.233*	*0.057*	*0.057*	*0.1890 ± 0.0005*	*19.8 ± 2.1*	*1*	*35*	*161*	-	-	-
dupl.§	2000	0.475	0.105	0.104	0.1767 ± 0.0001	22.1 ± 0.2	0	0	110	-	-	-
dupl.§	1022	0.131	0.098	0.098	0.1776 ± 0.0001	6.5 ± 0.3	1	1	401	-	-	-
dupl.§	1082	0.124	0.099	0.099	0.1769 ± 0.0001	6.0 ± 0.2	0	0	424	-	-	-
dupl.§§	1016	0.102	-	-	-	-	-	2	-	-	-	-
Silicates												
Garnet	24.53	7.2	0.048	0.048	0.168 ± 0.002	722 ± 21	1	1	3	0	3	147
Saussurite	21.75	0.075	0.005	0.005	0.210 ± 0.011	68 ± 20	10	9	65	35	4	26
Saussurite	95.04	0.14	0.010	0.010	0.446 ± 0.003	66 ± 2	5	52	282	252	7	33
Omphacite	16.38	0.30	0.033	0.033	0.214 ± 0.003	45 ± 3	2	20	104	59	1	2
Glaucophane	88.12	0.13	0.091	0.091	0.175 ± 0.001	6.8 ± 0.2	1	10	355	44	15	9
Talc	6.36	0.35	0.15	0.15	0.177 ± 0.004	11 ± 2	1	49	223	38	11	13
Sulphides	(µg)											
Sulphide	1793	14.7	31.5	31.3	0.184 ± 0.001	2.3 ± 0.1	1	4	1525	465	47	8
Sulphide	2750	28.2	0.49	0.48	0.367 ± 0.010	285 ± 17	21	1	48	42	0.7	15
Sulphide	1135	101	2.23	2.21	0.181 ± 0.001	220 ± 7	13	1	12	3	3	52
Sulphide	620.0	53.7	0.41	0.41	0.718 ± 0.021	672 ± 20	5	4	52	49	0.7	28
Sulphide	200.0	71.6	0.37	0.36	1.21 ± 0.14	1056 ± 132	15	9	61	59	0.6	38
Sulphide[m]	69.80	-	15.3	15.1	0.204 ± 0.003	-	1	-	-	-	23	-
Sulphide[m]	59.60	-	1.30	1.26	0.380 ± 0.033	-	11	-	-	-	2	-
S01/39ix												
Whole rock	2118	-	0.0053	0.0052	0.2187 ± 0.0140	-	4	-	-	-	-	-
Silicates												
Garnet	24.53	1.01	0.008	0.008	0.157 ± 0.003	580 ± 17	3	3	2	0	-	-
Cr-omphacite	35.32	-	0.013	0.013	0.148 ± 0.003	6.6 ± 3.0	3	-	-	-	-	-
Talc	16.52	0.60	0.020	0.019	0.197 ± 0.005	149 ± 24	4	18	25	15	-	-
Chloritoid	14.62	0.15	0.004	0.004	0.491 ± 0.034	163 ± 34	16	37	105	98	-	-
Sulphides	(µg)											
Sulphide	930.0	95.9	0.41	0.374	0.974 ± 0.010	1236 ± 37	3	1	41	40	-	-

Notes: See notes in Table 2 for Os* and uncertainties.
Blank (%)[‡] - the % contribution of the total procedural blank to the total Os or Re measured
Model age[a] – see Table 2; Model age[b] - calculated using an initial $^{187}Os/^{188}Os$ of 0.17, corresponding to the whole rock ratio at 45 Ma.
Prop. W.R.(%)[#] - the proportion of the whole rock budget of Os and Re which would be hosted by each phase, based on each individual measurement of the Os and Re concentration, hence the total is >>100%. An estimation of the 'true' average contribution of each phase has been made and is presented in Figure 11, and is discussed in the text.
Data in italics – previously published in Dale et al., (2007).
dupl. - Replicate analysis of the same powder, through repeated HF-HBr dissolution chemistry.
dupl.[§] - Replicate analysis of the same powder, through repeated high-pressure asher (HPA) digestion and chemistry.
dupl.[§§] - Replicate analysis of the same powder, through repeated HPA digestion and chemistry, including an initial HF-HCl desilicification step.
Sulphide[m] – Digestion and purification by microdistillation only.

Figure 1

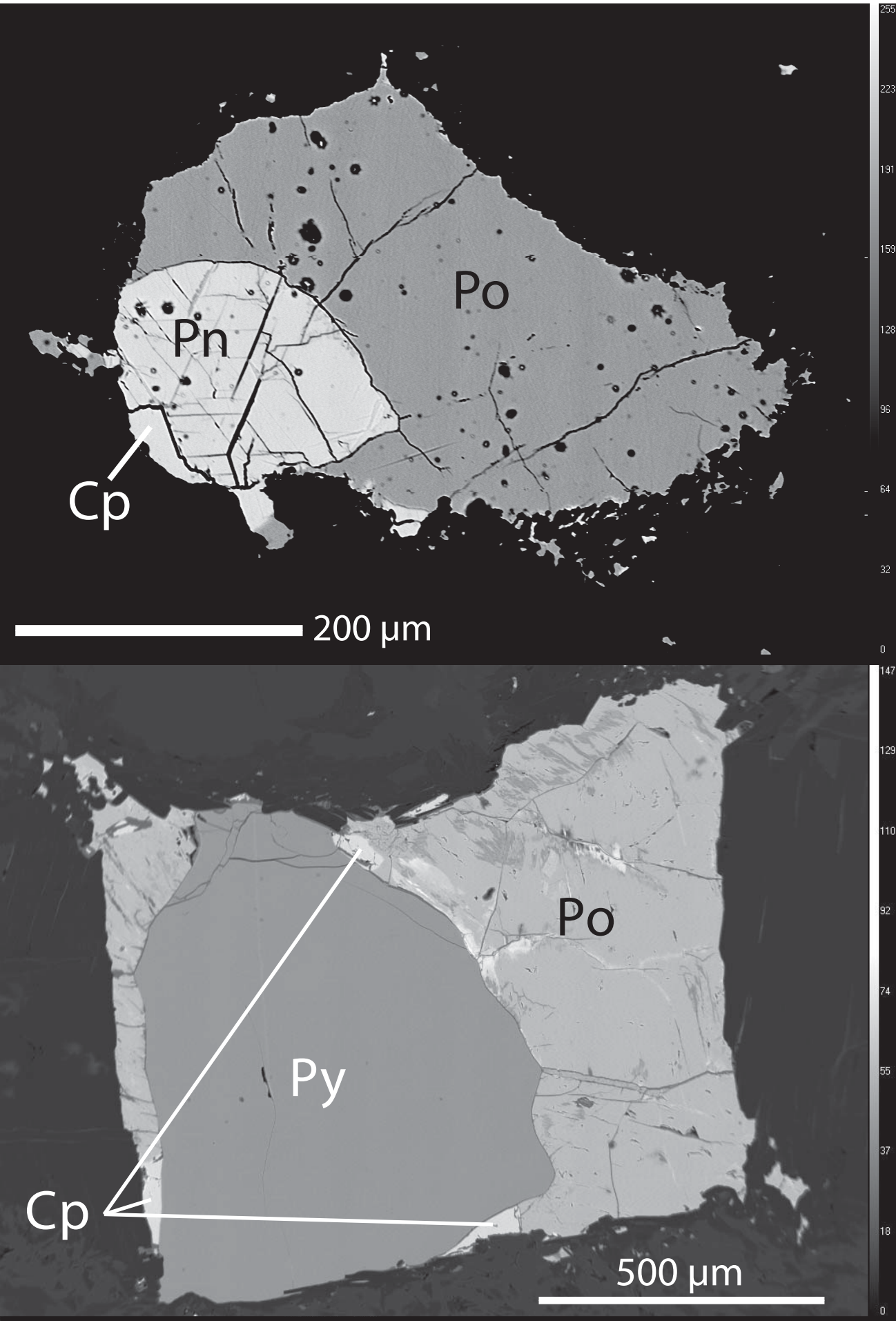

Figure 2

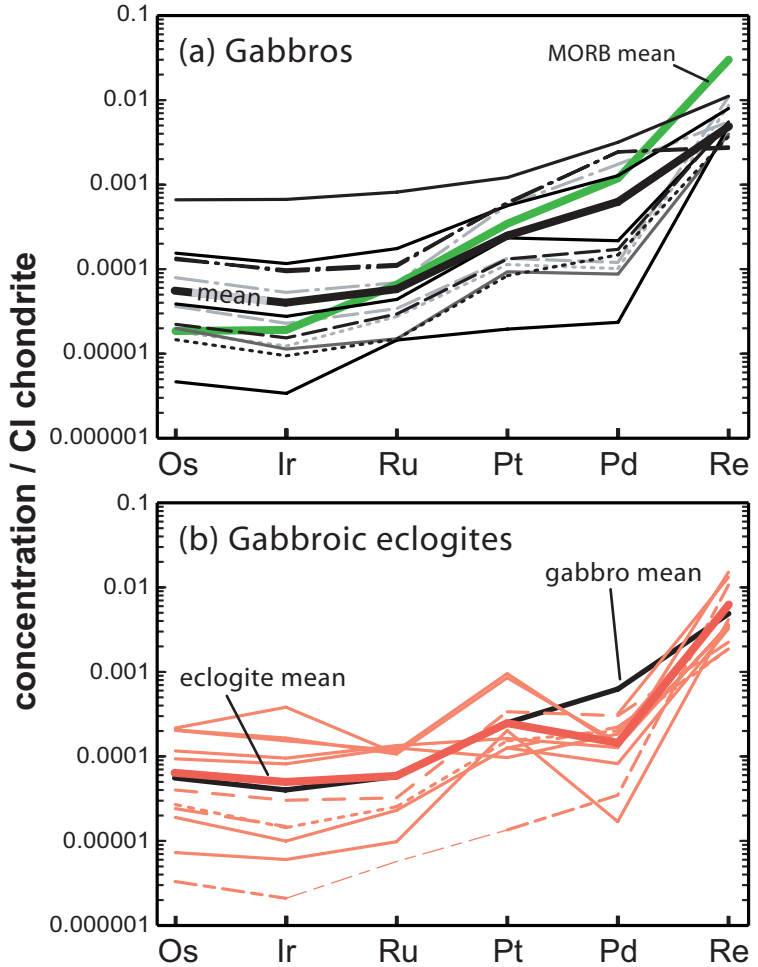

Figure 3

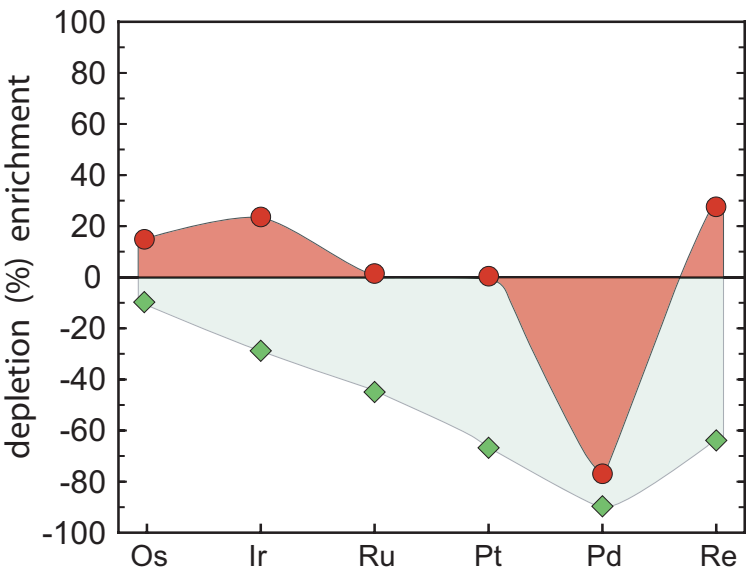

Figure 4

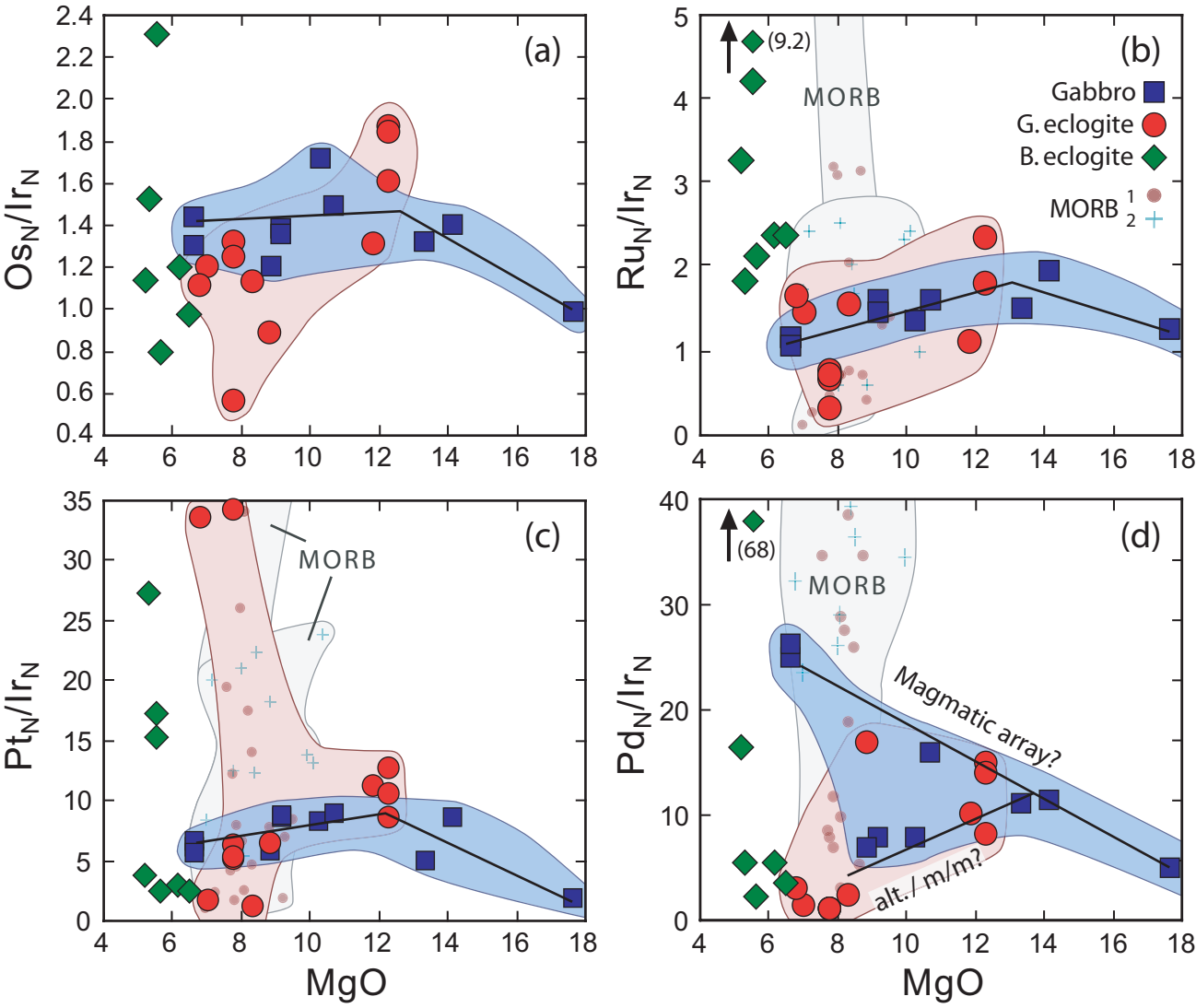

Figure 5

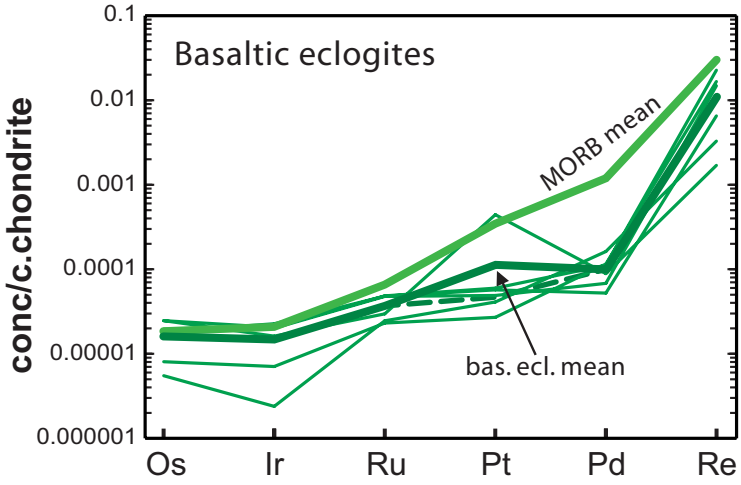

Figure 6

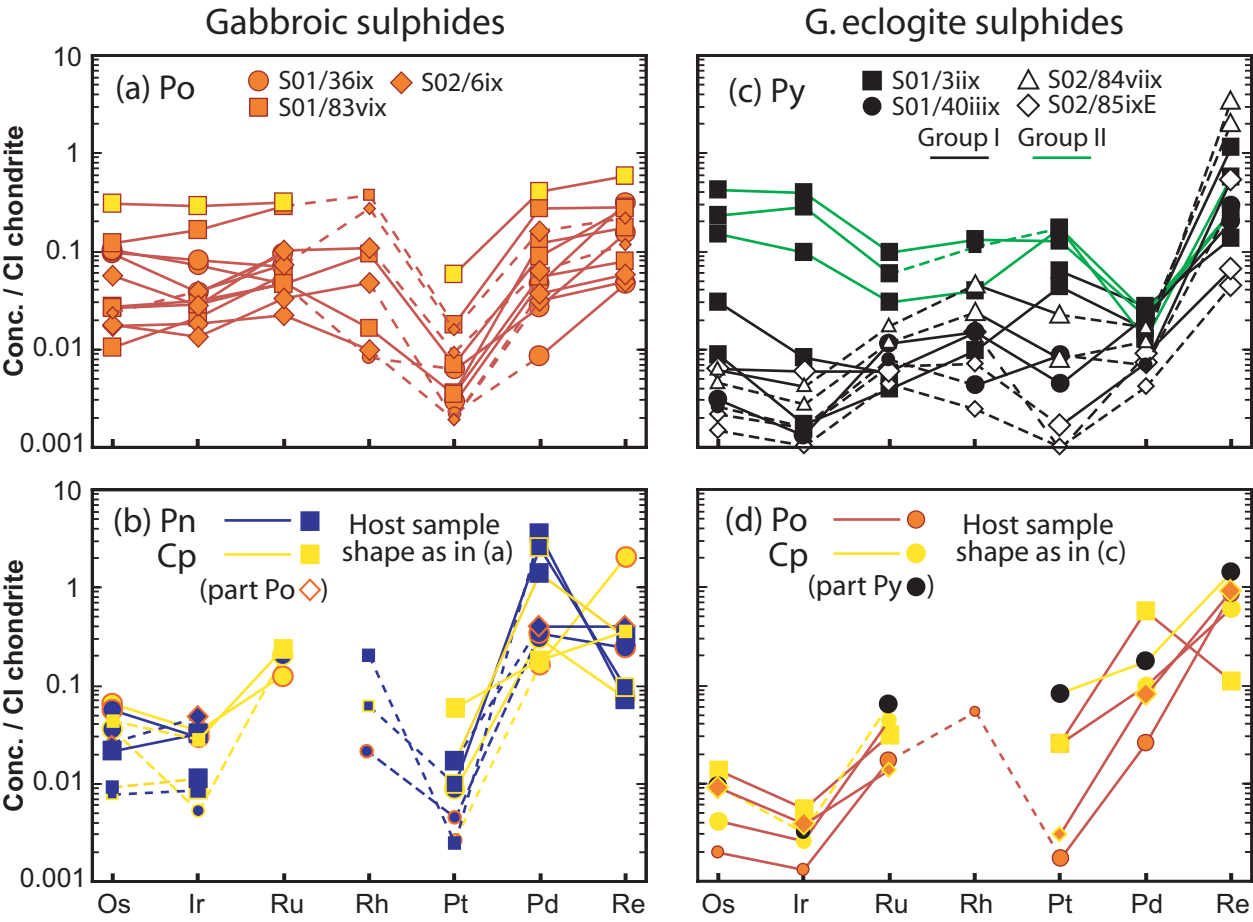
Gabbroic sulphides
G. eclogite sulphides
(a) Po
S01/36ix
S02/6ix
S01/83vix
(c) Py
S01/3iix
S01/40iiix
S02/84viix
S02/85ixE
Group I
Group II
(b) Pn
Cp
(part Po)
Host sample
shape as in (a)
(d) Po
Cp
(part Py)
Host sample
shape as in (c)
Conc. / CI chondrite
10
1
0.1
0.01
0.001
Os
Ir
Ru
Rh
Pt
Pd
Re

Figure 7

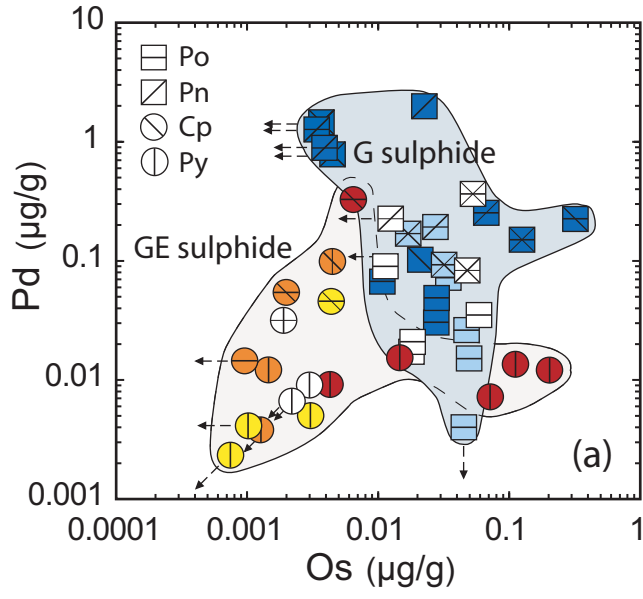
Po
Pn
Cp
Py
G sulphide
GE sulphide
(a)
Pd (µg/g)
Os (µg/g)
10
1
0.1
0.01
0.001
0.0001
0.001
0.01
0.1
1

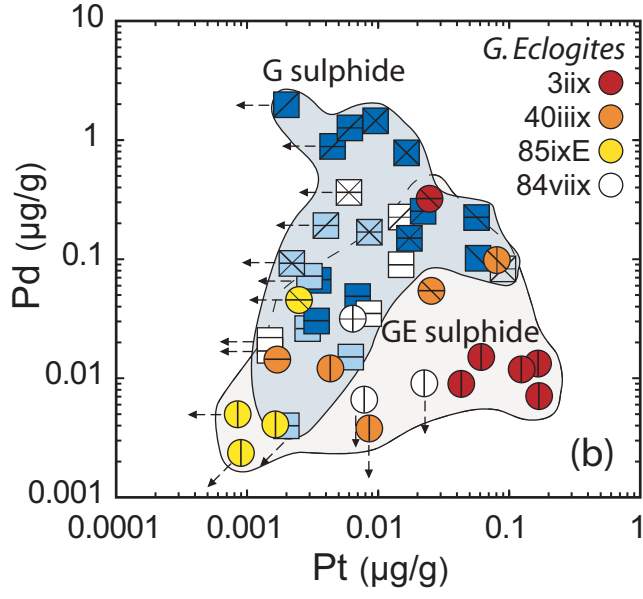
G. Eclogites
3iix
40iiix
85ixE
84viix
G sulphide
GE sulphide
(b)
Pd (µg/g)
Pt (µg/g)
10
1
0.1
0.01
0.001
0.0001
0.001
0.01
0.1
1

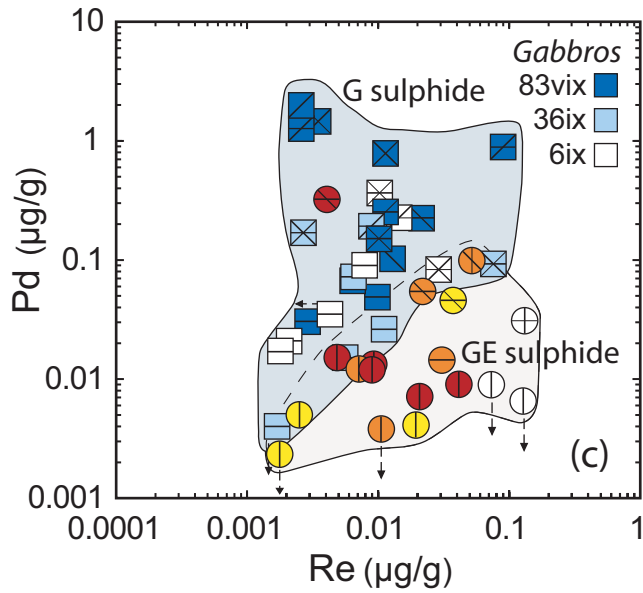
Gabbros
83vix
36ix
6ix
G sulphide
GE sulphide
(c)
Pd (µg/g)
Re (µg/g)
10
1
0.1
0.01
0.001
0.0001
0.001
0.01
0.1
1

Figure 8

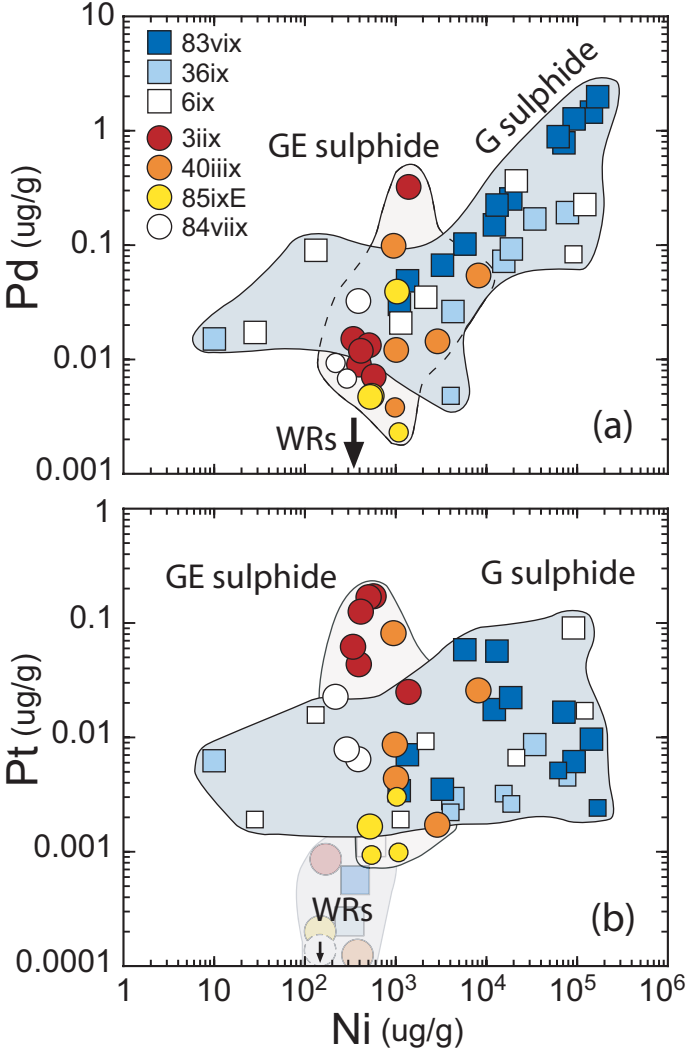
83vix
36ix
6ix
3iix
40iiix
85ixE
84viix
GE sulphide
G sulphide
WRs
(a)
Pd (ug/g)
10
1
0.1
0.01
0.001
GE sulphide
G sulphide
WRs
(b)
Pt (ug/g)
1
0.1
0.01
0.001
0.0001
1
10
10²
10³
10⁴
10⁵
10⁶
Ni (ug/g)

Figure 9

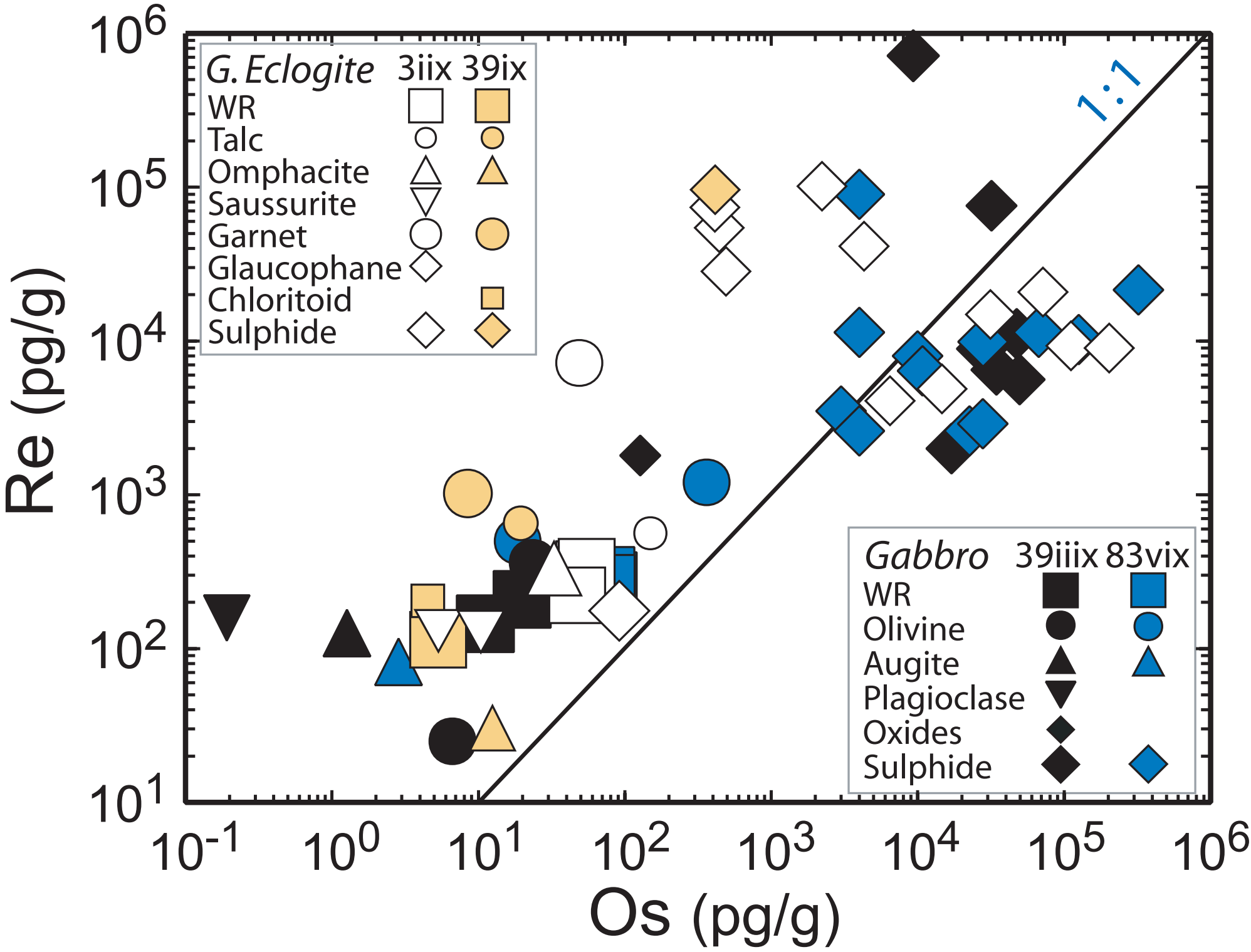
Re (pg/g)
Os (pg/g)
10^{6}
10^{5}
10^{4}
10^{3}
10^{2}
10^{1}
10^{-1}
10^{0}
10^{1}
10^{2}
10^{3}
10^{4}
10^{5}
10^{6}
1:1
G. Eclogite 3iix 39ix
WR
Talc
Omphacite
Saussurite
Garnet
Glaucophane
Chloritoid
Sulphide
Gabbro 39iiix 83vix
WR
Olivine
Augite
Plagioclase
Oxides
Sulphide

Figure 10

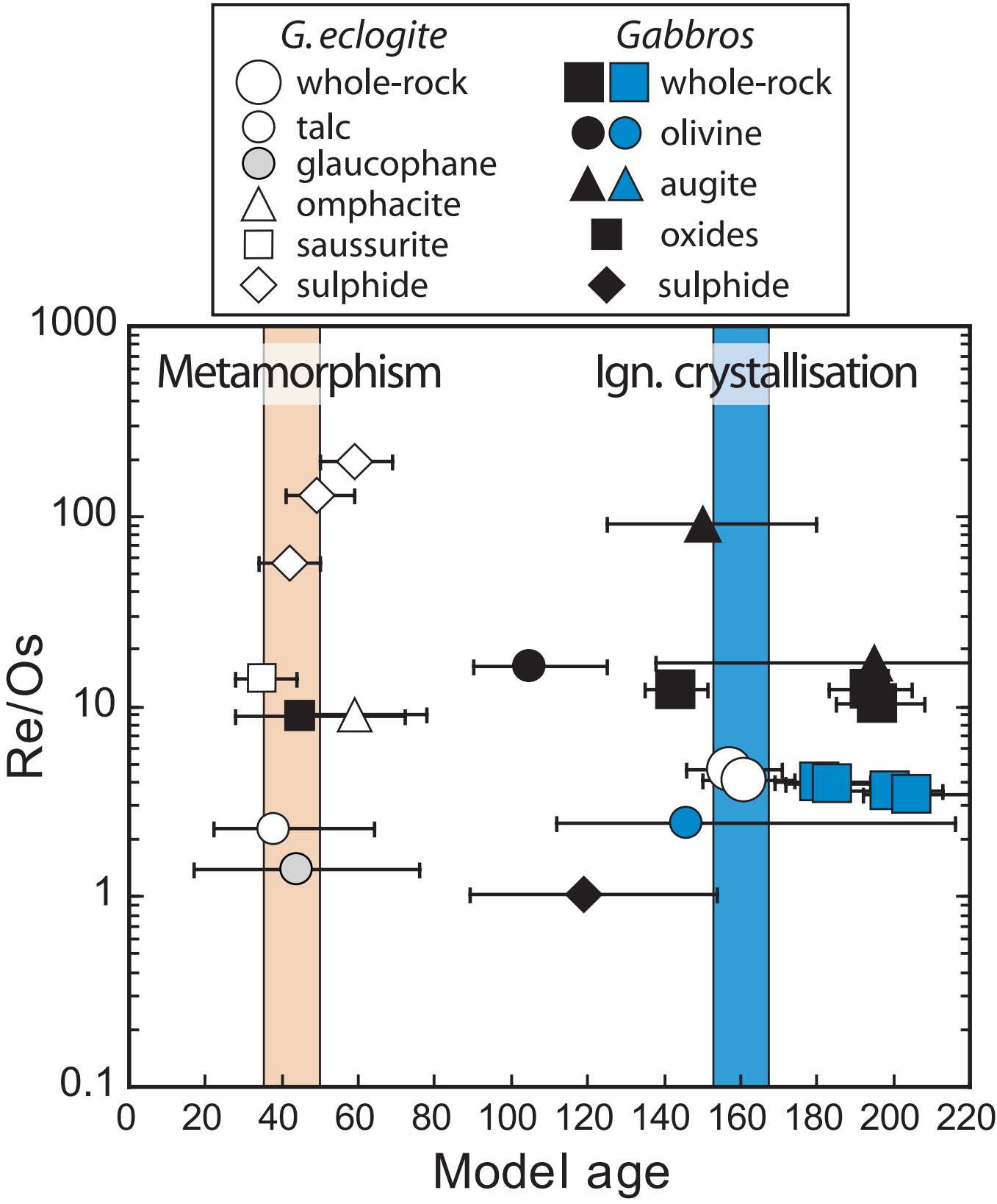
G. eclogite
whole-rock
talc
glaucophane
omphacite
saussurite
sulphide
Gabbros
whole-rock
olivine
augite
oxides
sulphide
Metamorphism
Ign. crystallisation
Re/Os
1000
100
10
1
0.1
0
20
40
60
80
100
120
140
160
180
200
220
Model age

Figure 11

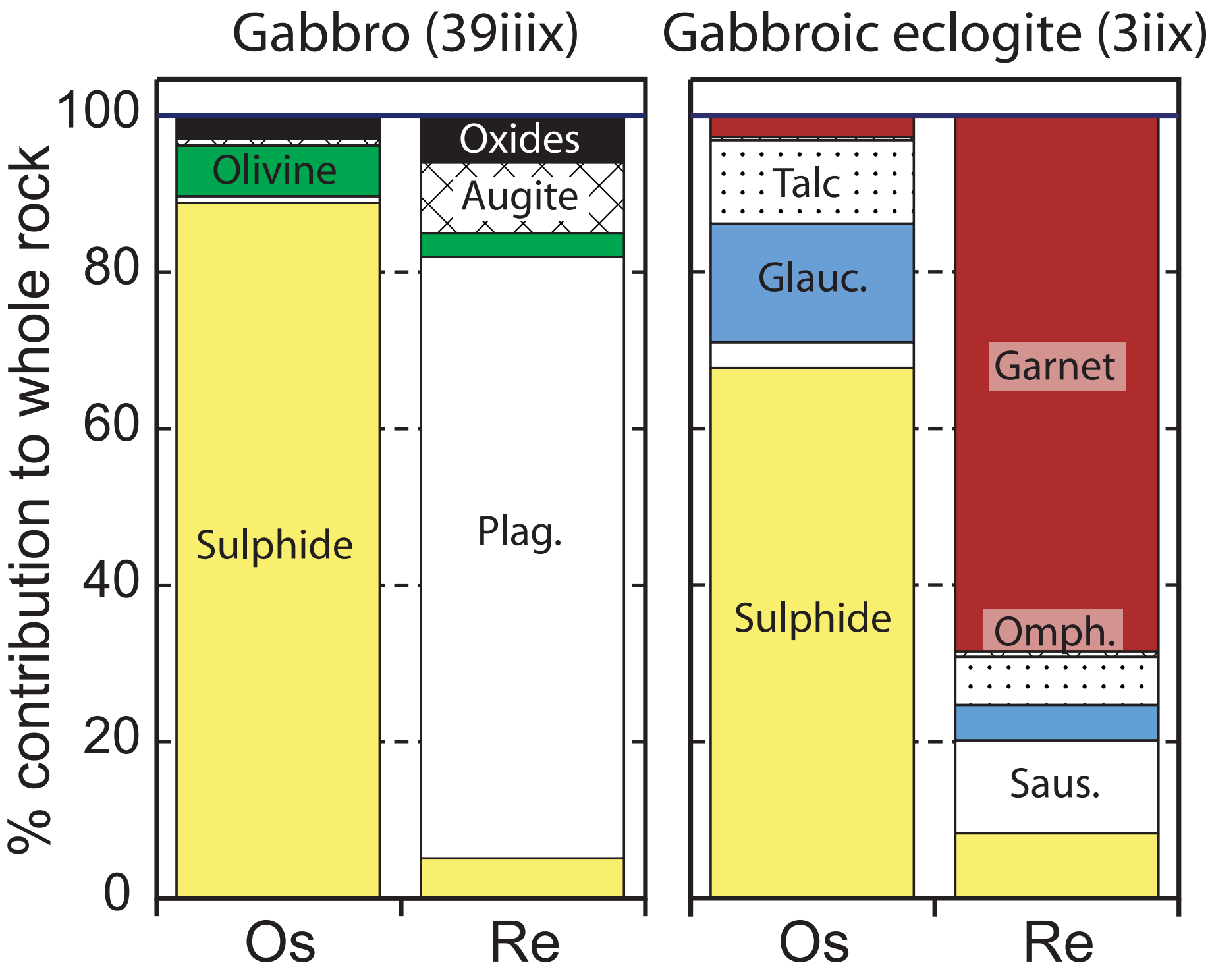
Gabbro (39iiix)
Gabbroic eclogite (3iix)
% contribution to whole rock
100
80
60
40
20
0
Olivine
Oxides
Augite
Sulphide
Plag.
Talc
Glauc.
Garnet
Sulphide
Omph.
Saus.
Os
Re
Os
Re

Figure 12

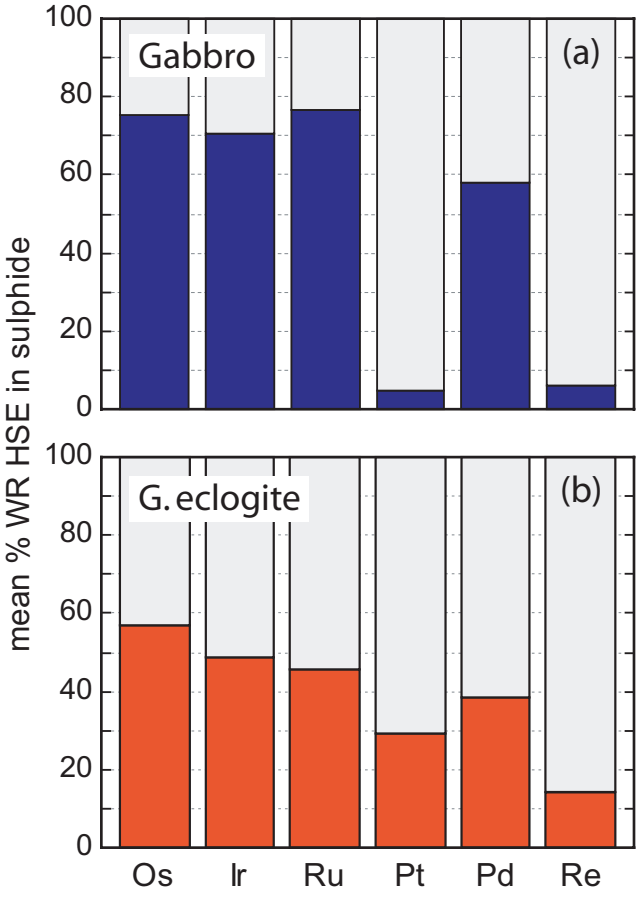

Figure 13